

See discussions, stats, and author profiles for this publication at: <https://www.researchgate.net/publication/48268026>

Control of a 2 D.O.F direct drive robot arm using integral sliding mode control

Article · October 2004

Source: OAI

CITATIONS

0

READS

2,740

1 author:

[Babul Salam KSM Kader Ibrahim](#)

Universiti Tun Hussein Onn Malaysia

74 PUBLICATIONS 395 CITATIONS

SEE PROFILE

Some of the authors of this publication are also working on these related projects:



EV Energy Management System [View project](#)

UNIVERSITI TEKNOLOGI MALAYSIA

BORANG PENGESAHAN STATUS TESIS •

**JUDUL: CONTROL OF A 2 D.O.F DIRECT DRIVE ROBOT ARM USING
INTEGRAL SLIDING MODE CONTROL**

SESI PENGAJIAN: 200-4/2005

Saya RABUL SALAM B. KSM KADER IBRAHIM

(HURUF BESAR)

mengaku membenarkan tesis (PSM/Sarjana/Doktor-Falsafah)* ini disimpan di Perpustakaan Universiti Teknologi Malaysia dengan syarat-syarat kegunaan seperti berikut:

1. Tesis adalah hakmilik Universiti Teknologi Malaysia.
2. Perpustakaan Universiti Teknologi Malaysia dibenarkan membuat salinan untuk tujuan pengajian sahaja.
3. Perpustakaan dibenarkan membuat salinan tesis ini sebagai pertukaran antara institusi pengajian tinggi.
4. **Sila tandakan (✓)

☐

SULIT

(Mengandungi maklumat yang berdarjah keselamatan atau kepentingan Malaysia seperti yang termaktub di dalam (AKTA RAHSIA RASMI 1972))

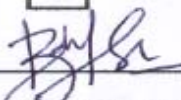
☐

TERHAD

(Mengandungi maklumat TERHAD yang telah ditentukan oleh organisasi/badan di mana penyelidikan dijalankan)

☒

TIDAK TERHAD


(TANDATANGAN PENULIS)

Disahkan oleh

(TANDATANGAN PENYELIA)

Alamat tetap:

**9, JALAN ANGGERIK 1,
TAMAN ROS, 86100
AYER HITAM, JOHOR.**

Nama Penyelia:

P.M. DR. MOHAMAD NOH B. AHMAD


Tarikh: 21 OCTOBER 2004

Tarikh: 21 OCTOBER 2004

CATATAN:

- Potong yang tidak berkenaan.
- Jika tesis ini SULIT atau TERHAD, sila lampirkan surat daripada pihak berkuasa/organisasi berkenaan dengan menyatakan sekali sebab dan tempoh tesis ini perlu dikelaskan sebagai SULIT atau TERHAD.
- ♦ Tesis dimaksudkan sebagai tesis bagi Ijazah Doktor Falsafah dan Sarjana secara penyelidikan, atau disertasi bagi pengajian secara kerja kursus dan penyelidikan, atau Laporan Projek Sarjana Muda (PSM).

“I hereby, declare that I have read this thesis and in my
opinion this thesis is sufficient in terms of scope
and quality for the award of degree of
Master of Engineering (Electrical-Mechatronics and Automatic Control)

Signature : 

Name of Supervisor : ASSOC. PROF DR. MOHAMAD NOH AHMAI

Date : 21 OCTOBER 2004

**CONTROL OF A 2 D.O.F DIRECT DRIVE ROBOT ARM USING
INTEGRAL SLIDING MODE CONTROL**

BABUL SALAM BIN KSM KADER IBRAHIM


**A project report submitted in partial fulfilment of the
requirements for a award of the degree of
Master of Engineering (Electrical-Mechatronics and Automatic Control)**

**Faculty of Electrical Engineering
Universiti Teknologi Malaysia**

OCTOBER, 2004

I declare that this thesis "Control of a 2 D.O.F Direct Drive Robot Arm using Integral Sliding Mode Control" is the result of my own research except for works that have been cited in the reference. The thesis has not been accepted any degree and not concurrently submitted in candidature of any other degree.

Signature

:  _____

Name of Author : BABUL SALAM B. KSM KADER IBRAHIM

Date

: 21 OCTOBER 2004

To my dearest father, mother and family for their encouragement and blessing

To my beloved be expecting wife for her support and caring

ACKNOWLEDGEMENT

First of all, I am greatly indebted to ALLAH SWT on His blessing to make this project successful.

I would like to express my gratitude to honourable Associate Professor Dr. Mohamad Noh Ahmad, my supervisor of Master's project. During the research, he helped me a lot especially in guiding to use Matlab/Simulink software. Then, during the discussion session, he tried to give me encouragement and assistance which finally leads me to the completion of this project.

Finally, I would like to dedicate my gratitude to my parents, my family, my lovely wife and my best friends who helped me directly or indirectly in the completion of this project. Their encouragement and guidance mean a lot to me. Their sharing and experience foster my belief in overcoming every obstacle encountered in this project.

Guidance, co-operation and encouragement from all people above are appreciated by me in sincere. Although I cannot repay the kindness from them, I would like to wish them to be well and happy always.

I am grateful to Kolej Universiti Teknologi Tun Hussein Onn (KUiTTHO), (my employer) for supporting me in the form of a scholarship and study leave.

ABSTRACT

High accuracy trajectory tracking is a very challenging topic in direct drive robot control. This is due to the nonlinearities and input couplings present in the dynamics of the robot arm. This thesis is concerned with the problems of modelling and control of a 2 degree of freedom direct drive arm. The research work is undertaken in the following five developmental stages; Firstly, the complete mathematical model of a 2 DOF direct drive robot arm including the dynamics of the brushless DC motors actuators in the state variable form is to be developed. In the second stage, the state variable model is to be decomposed into an uncertain model. Then, the Integral Sliding Mode Controller is applied to the robot arm. In the forth stage, perform the simulation. This is done through the simulation on the digital computer using MATLAB/SIMULINK as the platform. Lastly, the performance of Integral Sliding Mode Controller is to be compared with an Independent Joint Linear Control.

ABSTRAK

. Penjejak trajektori yang berketepatan tinggi merupakan satu topik yang mencabar dalam kawalan robot pacuan terus. Ini adalah disebabkan oleh ketaklelurusan dan gandingan masukan yang wujud di dalam dinamik lengan robot. Tesis ini membincangkan mengenai masalah dalam permodelan dan kawalan lengan robot yang mempunyai 2 darjah kebebasan. Kajian ini melibatkan lima peringkat seperti berikut; Pertama, pembangunan model matematik 2 DOF lengan robot pacuan terus yang lengkap merangkumi dinamik pemacu motor DC tanpa berus dalam bentuk pembolehubah keadaan. Di peringkat kedua, model pembolehubah keadaan akan dipisahkan ke model yang tidak tetap. Kemudian, kawalan ragam gelincir kamiran diguna pakai dalam lengan robot ini. Peringkat kelima adalah membuat penyelakuan. Simulasi atau penyelakuan ini dijalankan menggunakan komputer digital dengan bantuan perisian MATLAB/SIMULINK. Akhir sekali, keupayaan di antara kawalan ragam gelincir kamiran dengan kawalan lurus bebas lipatan dibandingkan.

CONTENTS

SUBJECT	PAGE
TITLE	i
DECLARATION	ii
DEDICATION	iii
ACKNOWLEDGEMENT	iv
ABSTRACT	v
ABSTRAK	vi
CONTENTS	vii
LIST OF TABLES	x
LIST OF FIGURES	xi
LIST OF SYMBOLS	xiii
LIST OF ABBREVIATIONS	xvi
 CHAPTER 1 INTRODUCTION	 1
1.1 Overview	1
1.2 Objective	2
1.3 Scope of Project	3
1.4 Research Methodology	3
1.5 Advantages and Disadvantages Direct Drive Robot Arm	4
1.6 Literature Review	5
1.7 Layout of Thesis	9

CHAPTER 2 MATHEMATICAL MODELLING	10
2.1 Introduction	10
2.2 Brushless DC Motor (BLDCM) Dynamics	11
2.3 Modelling of Robot Dynamics	16
2.4 The Complete Integrated Model	21
 CHAPTER 3 INTEGRAL SLIDING MODE CONTROL DESIGN	 25
3.1 Overview of Controller	25
3.2 Introduction to Variable Structure Control (VSC) with sliding mode control	26
3.2 Decomposition Into An Uncertain Systems	28
3.3 Problem Formulation	31
3.4 System Dynamics During Sliding Mode	33
3.5 Sliding Mode Tracking Controller Design	34
 CHAPTER 4 SIMULATION RESULTS	 37
4.1 Introduction	37
4.2 Trajectory Generation	38
4.3 Simulation Using Independent Joint Linear Control (IJC)	41
4.4 Simulation Using Integrated Sliding Mode Controller	
4.4.1 The Selection of Controller Parameters	44
4.4.2 Numerical Computation	47
4.4.3 The Effect of the Value of Controller Parameter, γ	49
4.5 Control Input Chattering Suppression	57

CHAPTER 5 CONCLUSION & FUTURE WORKS	65
5.1 Conclusion	65
5.1 Suggestion For Future Work	66
REFERENCES	67

LIST OF TABLES

TABLE NUMBER	TITLE	PAGE
1.1	Advantages and Disadvantages of Direct Drive Robot	5
2.1	Parameters of the Actuators for Robot Arm	15
2.2	List of Parameters of Robot Arm	16
3.1	Value of Elements in Matrices $A(x,t)$ and $B(x,t)$	29
4.1	Two Sets of Controller Parameters	49
4.2.	Continuous Function Constants	59

LIST OF FIGURES

FIGURE NUMBER	TITLE	PAGE
2.1	2 DOF Direct Drive Robot Arm [Reyes & Kelly,2001]	11
2.2	Block Diagram of The Position Control of Each Joint of Robot	12
2.3	Block Diagram of the BLDCM	12
2.4	A Configuration of 2 DOF Direct Drive Robot Arm [Reyes&Kelly, 2001]	16
3.1	Overview of Control Structure	25
4.1	Desired Joint Position Profile For Both Joints	38
4.2	Desired Joint Velocity Profile For Both Joints	39
4.3	Desired Joint Acceleration Profile For Both Joints	40
4.4	Tracking Response of Joint 1 with IJC	43
4.5	Tracking Response of Joint 2 with IJC	43
4.6	Tracking Response of Joint 1 with Unsatisfied Controller Parameters	50
4.7	Tracking Response of Joint 2 with Unsatisfied Controller Parameters	50
4.8	Joint 1 Control Input of PISMC with Unsatisfied Controller Parameters	51
4.9	Joint 2 Control Input of PISMC with Unsatisfied Controller Parameters	51

4.10	Joint 1 Sliding Surface of PISMC with Unsatisfied Controller Parameters	52
4.11	Joint 2 Sliding Surface of PISMC with Unsatisfied Controller Parameters	52
4.12	Tracking Response of Joint 1 with Satisfied Controller Parameters	53
4.13	Tracking Response of Joint 2 with Satisfied Controller Parameters	54
4.14	Joint 1 Control Input of PISMC with Satisfied Controller Parameters	54
4.15	Joint 2 Control Input of PISMC with Satisfied Controller Parameters	55
4.16	Joint 1 Sliding Surface of PISMC with Satisfied Controller Parameters	55
4.17	Joint 2 Sliding Surface of PISMC with Satisfied Controller Parameters	56
4.18	Phenomenon of Chattering	57
4.19	Continuous Function	59
4.20	Joint 1 Control Input Using PISMC Tracking Controller with Discontinuous Function	60
4.21	Joint 2 Control Input Using PISMC Tracking Controller with Discontinuous Function	61
4.22	Joint 1 Control Input Using PISMC Tracking Controller with Continuous Function	62
4.23	Joint 2 Control Input Using PISMC Tracking Controller with Continuous Function	63
4.24	Joint 1 Tracking Error Using PISMC Tracking Controller with Continuous Function	64
4.25	Joint 2 Tracking Error Using PISMC Tracking Controller with Continuous Function	65

LIST OF SYMBOLS

<u>SYMBOL</u>	<u>DESCRIPTION</u>
1. UPPERCASE	
$A(*,*)$	2N x 2N system matrix for the integrated direct drive robot arm
A_{ac}	2N x 2N system matrix for the augmented dynamic equation of the actuators
$\Delta A(*,*)$	matrix representing the uncertainties in the system matrix
$B(*,*)$	2N x N input matrix for the integrated direct drive robot arm
B_{ac}	2N x N input matrix for the augmented dynamic equation of the actuators
$\Delta B(*,*)$	matrix representing the uncertainties in the input matrix
C	N x 2N constant matrix of the PI sliding surface
$E(*)$	a continuous function related to $\Delta B(*,*)$
F_i	motor damping constant (kg.m ² /s)
$H(*)$	a continuous function related to $\Delta A(*,*)$
I^*	brushless DC motor demand current
I_{DC}	brushless DC motor DC supply current
J_i	moment of inertia of the i th motor (kg.m ²)
K_i	linear feedback gain matrix for the i th sub-system
K_t	motor torque constant (N.m/A)
L_{s_i}	stator winding inductance for i th motor (H)
N	number of joints
Q	2N x N load distribution matrix for the augmented dynamic equation of the actuators

R_{s_i}	stator winding resistance for i th motor (Ω)
\Re^N	N -dimensional real space
$S_\delta(t)$	a continuous function used to eliminate chattering
T_{L_i}	load torque for i th motor (N.m)
$U(*)$	$N \times 1$ control input vector for a N DOF robot arm
$X(*)$	$2N \times 1$ state vector for the integrated direct drive robot arm
$Z(*)$	$2N \times 1$ error state vector between the actual and the desired states of the overall system
$(*)^T$	transpose of $(*)$
$\ (*)^T\ $	Euclidean norm of $(*)$

2. LOWERCASE

a_{ij}	ij th element of the integrated system matrix $A(*,*)$
b_{ij}	ij th element of the integrated input matrix $B(*,*)$
g	gravity acceleration ($m.s^2$)
l_i	length of the i th manipulator link (m)
m_i	mass of the i th manipulator link (kg)
t	time (s)

3. GREEK SYMBOLS

α	norm bound of continuous function $H(*)$
β	norm bound of continuous function $E(*)$
$\dot{\theta}$	joint displacement (rad)
$\ddot{\theta}$	joint velocity (rad/s)
$\ddot{\theta}$	joint acceleration (rad/s^2)
$\dot{\theta}_d$	desired joint angle (rad)

$\dot{\theta}_d$	desired joint velocity (rad/s)
$\ddot{\theta}_d$	desired joint acceleration (rad/s ²)
σ	Integral sliding manifold
τ	time interval for arm to travel from a given initial position to a final desired position (seconds)

LIST OF ABBREVIATIONS

AC	Alternating Current
BLDCM	Brushless Direct Current Motor
DC	Direct Current
DOF	Degree of Freedom
IJC	Independent Joint Control
LHP	Left Half Plane
SMC	Sliding Mode Control
VSC	Variable Structure Control
VSS	Variable Structure System

CHAPTER 1

INTRODUCTION

1.1 Overview

High accuracy trajectory tracking is a very challenging topic in direct drive robot control. This is due to the nonlinearities and input couplings present in the dynamics of the arm. This thesis presents the modelling and control of a 2 DOF (degree of freedom) direct drive robot arm. Direct drive robot arm is mechanical arm in which the shafts of articulated joints are directly coupled to the rotors of motors with high torque. Therefore, it does not contain transmission mechanisms between motors and their load.

Serial kinematics chains have made up the majority of robot manipulator designs. Serious difficulties with serial mechanisms have proven difficult to overcome. High torques must be generated in the joints due to relatively long moment arms. Hydraulic actuators gave high force to weight ratios, but introduced maintenance and safety concerns. Electrical drives using gear trains, shafts, and couplings, could provide the necessary joint torques. However, these driving components introduced friction which reduced force control capabilities, and

backlash which reduced precision. Manipulator stiffness is also reduced by these drive components which are sometimes introduced to reduce the inertia of the links. Direct drive (DD) serial manipulators were introduced in the 1980's as a proposed solution to many of these problems [Asada and Kanade, 1983].

The direct drive joint consists of a pair of arm links, the motor, and the bearings. The motor is comprised of a stator and a rotor. The stator is housed in the case connected to a proximal link, and the rotor is directly coupled to the joint shaft, which is connected to the other arm link at a distal link. Thus the distal arm link is rotated directly by the torque exerted between the rotor and the stator, hence direct drive. Throughout this project, a two DOF direct-drive robot manipulator driven by Brushless DC Motors (BLDCM) is considered.

1.2 Objective

The objectives of this research are as follows:

1. To formulate the complete mathematical dynamic model of the BLDCM driven direct drive revolute robot arm in state variable form. The complete model will be made available by integrating the dynamics of the 2 DOF direct drive robot arm with the BLDCM dynamics
2. To transform the integrated nonlinear dynamic model of the BLDCM driven direct drive robots into a set of nonlinear uncertain model comprising the nominal values and the bounded uncertainties. These structured uncertainties exist due to the limit of the angular positions, speeds, and accelerations.
3. To control the 2 DOF direct drive robot using Integral Sliding Mode Controller and to compare the performance between Integral SMC with other conventional controller.

1.3 Scope of Project

The scopes of work for this project are

- The use of a 2 DOF Brushless DC motor driven Direct Drive Robot Arm as described in Reyes and Keyes(2001).
- Simulation work using MATLAB/Simulink as platform.

- The use of Integral Sliding Mode Controller as described in Ahmad et al.(2002).
- The comparison of the performance of Integral Sliding Mode Controller with Independent Joint Linear Control.

1.3 Research Methodology

The research work is undertaken in the following five developmental stages:

- a) Development of the complete mathematical model of a 2 DOF direct drive robot arm including the dynamics of the Brushless DC Motors actuators in the state variable form.
- b) Decomposition of the complete model into an uncertain model.
- c) Utilize Integral Sliding Mode Controller as robot arm controller.
- d) Perform simulation of this controller in controlling a 2 DOF direct drive robot arm. This simulation work will be carried out on MATLAB platform with Simulink as it user interface.
- e) Compare of the performance of Integral Sliding Mode Controller with other controller such as Independent Joint Linear Control.

1.5 Advantages and Disadvantages of Direct Drive Robot Arm

Positioning inaccuracy and tuning challenges are common in such systems due to transmission compliance and backlash. A direct drive rotary motor is simply a high torque permanent magnet motor that is directly coupled to the load. This design eliminates all mechanical transmission components such as gearboxes, belts, pulleys and couplings. Direct drive rotary systems offer a number of unique and significant advantages to the designer and user. Because a mechanical transmission requires constant maintenance and frequently causes unscheduled down time, direct drive rotary motors inherently increase machine reliability and reduce maintenance time and expense. By eliminating compliance in the mechanical transmission, the need for inertia matching of the motor to the load is eliminated, while position and velocity accuracy can be increased by up to 50 times [Asada and Toumi, 1987].

Direct-drive technique eliminates the problems associated with gear backlash as well as reducing the friction significantly. Moreover, the mechanical construction is much stiffer than the conventional robot manipulator with gearing, wear and tear is not a problem, and the construction is more reliable and easy to maintain due to its simplicity. These features make the direct drive robots suitable for the high-speed application of industrial robot such as the laser cutting application.

A key factor for direct drive robot performance is the torque to mass ratio of the actuators. Direct drive robots had their own sets of difficulties. It cannot be controlled by simple controller due to the non linear coupled dynamic and input couplings.

The advantages and disadvantages of direct drive robot can be summarized as in Table 1.1.

Table 1.1 : Advantages and Disadvantages of Direct Drive Robot

ADVANTAGES	DISADVANTAGES
<ul style="list-style-type: none">▪ No gear backlash and lower friction.▪ Simpler construction.▪ No wear and tear▪ Fast and accurate	<ul style="list-style-type: none">▪ Very non linear coupled dynamic▪ Consist of uncertainties▪ Input couplings▪ Cannot be controlled by simple controller

1.6 Literature Review

The purpose of manipulator control is to maintain the dynamic response of a manipulator in accordance with pre-specified objectives. The dynamic performance of a manipulator directly depends on the efficiency of the control algorithms and the dynamic model of the manipulator. Most of current industrial approaches to the robot arm control design treat each joint of the manipulator as a simple linear servomechanism with simple controller like Independent Joint Control (IJC), proportional plus derivative (PD), or proportional plus integral plus derivative (PID) controllers. In this approach, the nonlinear, coupled and time-varying dynamics of the mechanical part of the robot manipulator system have usually been completely ignored, or assumed as disturbances. However, when the links are moving simultaneously and at high speed, the nonlinear coupling effects and the interaction forces between the manipulator links may decrease the performance of the overall system and increase the tracking error. The disturbances and uncertainties such as variable payload in a task cycle may also reduce the tracking quality of the robot manipulator system [Osman, 1991].

Since the early days of the robot, robot control system has become an active

research area. Various advanced and sophisticated control strategies have been proposed by numerous researchers for controlling the robot manipulator such that the system is stable as well as the motion of the manipulator arm is maintained along the prescribed trajectory. The structures of these controllers can be grouped into three categories, the centralized, decentralized, and multilevel hierarchical structures. Many strategies have been developed for the centralized control schemes for improving the control of the nonlinear and coupled time varying robot manipulator. These include among others, the Computed Torque techniques [Craig, 1989], Adaptive control strategies [Ortega and Spong, 1988] and the Variable Structure Control approaches [Young, 1978].

Variable Structure Control (VSC) with sliding mode control was first proposed and elaborated in the early 1950's in the Soviet Union by Emelyanov and several co-researchers. Since 1980, two developments have greatly enhanced the attention given to VSC systems. The first is the existence of a general VSC design method for complex systems. The second is a full recognition of the property of perfect robustness of a VSC system with respect to system perturbation and disturbances [John and James, 1993].

A sliding mode will exist for a system if in the vicinity of the switching surface, the state vector is directed towards the surface. Filippov's method is one possible technique for determining the system motion in a sliding mode, but a more straight forward technique easily applicable to multi-input systems is the method of equivalent control, as proposed by Utkin and Drazenovic [DeCarlo, et. al 1988].

The motivation for exploring uncertain systems is the fact that model identification of real world systems introduced parameter errors. Hence models contain uncertain parameters which are often known to lie within upper and lower bounds. A whole body of literature has risen in recent years concerned with the deterministic stabilization of systems having uncertain parameters lying within

known bounds. Such control strategies are based on the second method of Lyapunov. One has to take notice that, the plant uncertainties are required to lie in the image of input matrix B for all values of t and x . This requirement is the so-called matching condition [Gao and Hung, 1993]. The physical meaning of matching condition is that all modeling uncertainties and disturbances enter the system through the control channel [John and James, 1993].

Sliding mode techniques are one approach to solving control problems and are an area of increasing interest. In the formulation of any control problem there will typically be discrepancies between the actual plant and the mathematical model developed for controller design. This mismatch may be due to any number of factors and it is the engineer's role to ensure the required performance levels exist despite the existence of plant/model mismatches. This has led to the development of so-called robust control methods. However this approach is decreasing the order of the system dynamics, may produce undesirable result in certain application. Other alternative must be introduced to increase the order of the closed-loop dynamics [Ahmad, 2003].

To overcome the problem of reduced order dynamics, a variety of the sliding mode control known as the Integral Sliding Mode Control has been successfully applied in a variety of control. Different from the conventional SMC design approaches, the order of the motion equation in ISMC is equal to the order of the original system, rather than reduced by the number of dimension of the control input. The method does not require the transformation of the original plant into the canonical form. Moreover, by using this approach, the robustness of the system can be guaranteed throughout the entire response of the system starting from the initial time instance [Ahmad, 2003].

1.7 Layout of Thesis

This thesis contained five chapters. Chapter 2 deals with the mathematical modelling of the direct drive robot arm. The formulation of the integrated dynamic model of this robot arm is presented. First, the state space representations of the actuator dynamics comprising of BLDCM motors are formulated. Then, the state space representations of the dynamic model of the mechanical linkage of the direct drive robot arm are established. Based on the actuator dynamics model, an integrated dynamic model of the robot arm is presented.

Chapter 3 presents the controller design using integral sliding mode control. The direct drive robot arm is treated as an uncertain system. Based on the allowable range of the position and velocity of the direct drive robot arms operation, the model comprising the nominal and bounded uncertain parts is computed. Then, a centralized control strategy for direct drive robot arm based on Integral Sliding Mode Control is described.

Chapter 4 discusses the simulation results. The performance of the Integral sliding mode controller is evaluated by simulation study using Matlab/Simulink. For the comparison purposes, the simulation study of Independent Joint Linear Control is also presented.

Chapter 5 summarizes the works undertaken. Recommendations for future work of this project are presented at the end of the chapter.

CHAPTER 2

MATHEMATICAL MODELING

2.1 Introduction

The most important initial step in the controlling an industrial robot is to obtain a complete and accurate mathematical model of the robot manipulator. This model is useful for computer simulation of the robot arm motion and synthesis processes before applied into real robot action.

The purpose of manipulator control is to maintain the dynamic response of a manipulator in accordance with pre-specified objectives. The dynamic performance of a manipulator directly depends on the efficiency of the control algorithms and the dynamic model of the manipulator [Ahmad, 2003]. Since the actuators are part of robot manipulator system, it is necessary to consider the effect of actuator dynamics. Therefore, it is important to include the actuators dynamic into the robot arm dynamic equations.

The formulation of an integrated mathematical dynamic model of an electrically driven direct drive robot arm is presented in this chapter. In this thesis, a

2DOF whose rigid links are jointed with revolute joints as shown in Figure 2.1 is considered. Both links of robot arm are actuated by brushless direct drive servo actuator BLDCM to drive the joints without gear reduction.

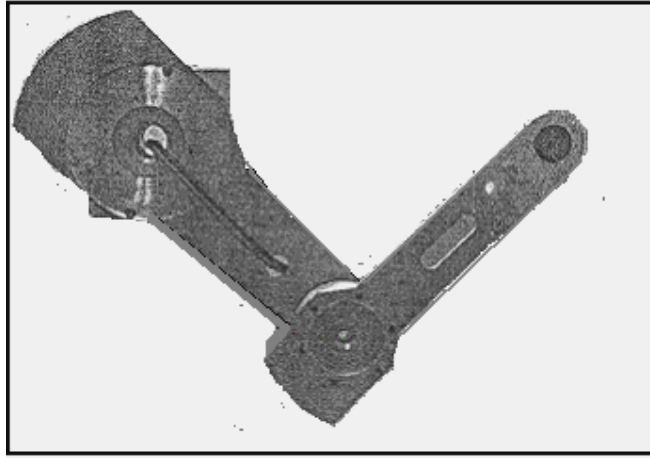


Figure 2.1 : 2 DOF Direct Drive Robot Arm [Reyes & Kelly,2001]

2.2 Brushless DC Motor (BLDCM) Dynamics

The 2 DOF direct drive robot considered in this thesis employed a BLDCM at each joint to drive the link. The block diagram of the position control of each joint of robot can be represented as shown in Figure 2.2. The control unit, Sliding Mode Controller is receiving position error, shaft speed and shaft acceleration as input and provides demand current for the current controller as the output.

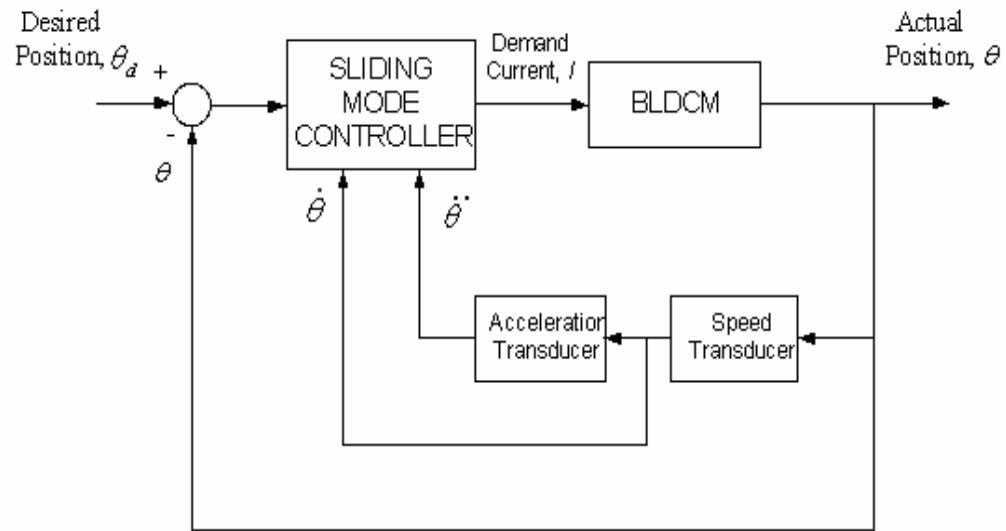


Figure 2.2 : Block Diagram of The Position Control of Each Joint of Robot

In order to proceed with the formulation of the integrated dynamic model of the direct drive robot manipulator, a complete set of dynamic equations of the actuators must be formulated first. The block diagram for the BLDCM as shown in Figure 2.2 is considered.

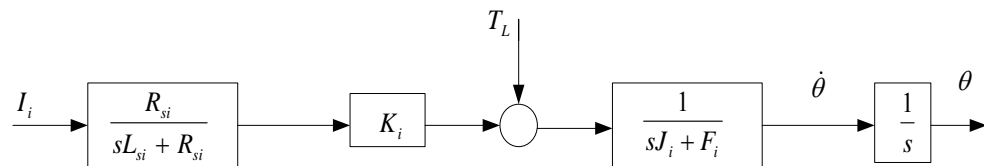


Figure 2.3 : Block Diagram of the BLDCM

From the block diagram of the actuator, the equations of motion for the BLDCM can be obtained as follows [Karunadasa and Renfrew, 1991]:

$$\dot{\theta}_i(t) = -\left(\frac{F_i}{J_i} + \frac{R_{si}}{L_{si}}\right)\ddot{\theta}_i(t) - \frac{F_i R_{si}}{J_i L_{si}}\dot{\theta}_i(t) + \frac{K_i R_{si}}{J_i L_{si}}I_i^*(t) - \frac{R_{si}}{J_i L_{si}}T_L(t) - \frac{1}{J_i}\dot{T}_L(t) \quad (2.1)$$

where

$\dot{\theta}$: motor position (rad)

$\ddot{\theta}$: motor velocity (rad/s)

$\ddot{\theta}$: motor acceleration (rad/s²)

R_{s_i} : motor stator winding resistance (Ω)

L_{s_i} : motor stator winding inductance (H)

K_t : motor torque constant (N.m/A)

J_i : motor rotor inertia (kg.m²)

F_i : motor damping constant (kg.m²/s)

I_i^* : motor demand current (A)

T_{L_i} : motor load torque (N.m)

Define a 2x1 state vector of the i th actuator as

$$X_i(t) = [\theta_i(t) \quad \dot{\theta}_i(t) \quad \ddot{\theta}_i(t)]^T \quad (2.2)$$

Then equation (2.1) can then be written in state variable form as

$$\dot{X}_i(t) = A_{ac_i} X_i(t) + B_{ac_i} U_i(t) + Q_i T_{L_i}(t) + W_i \dot{T}_{L_i}(t) \quad (2.3)$$

where,

$$A_{aci} = \begin{bmatrix} 0 & 0 & 1 \\ 0 & -\frac{F_i R_{si}}{J_i L_{si}} & -\left(\frac{F_i}{J_i} + \frac{R_{si}}{L_{si}}\right) \end{bmatrix}, \quad B_{aci} = \begin{bmatrix} 0 \\ \frac{K_i R_{si}}{J_i L_{si}} \end{bmatrix}$$

$$Q_i = \begin{bmatrix} 0 \\ -\frac{R_{si}}{J_i L_{si}} \end{bmatrix}, \quad W_i = \begin{bmatrix} 0 \\ -\frac{1}{J_i} \end{bmatrix}, \quad U_i(t) = I_i^*(t) \quad (2.4)$$

with $X_i(t)$ is a 2 x 1 state vector and $U_i(t)$ is a scalar input of the i th actuator, while $T_{Li}(t)$ is the load acting on the i th actuator due to the manipulator links.

For a 2 DOF direct drive robot manipulator, the augmented dynamic equation of the actuators can be written in compact form as follows:

$$\dot{X}(t) = A_{ac} X(t) + B_{ac} U(t) + Q T_L(t) + W \dot{T}_L(t) \quad (2.5)$$

where,

$$X(t) = [X_1^T(t) \quad X_2^T(t)]^T$$

$$U(t) = [U_1(t) \quad U_2(t)]^T$$

$$T_L(t) = [T_{L1}(t) \quad T_{L2}(t)]^T$$

$$\dot{T}_L(t) = [\dot{T}_{L1}(t) \quad \dot{T}_{L2}(t)]^T$$

$$A_{ac} = \text{diag}[A_{ac1} \quad A_{ac2}]$$

$$B_{ac} = \text{diag}[B_{ac1} \quad B_{ac2}]$$

$$Q(t) = \text{diag}[Q_1(t) \quad Q_2(t)]$$

$$W(t) = \text{diag}[W_1(t) \quad W_2(t)]$$

Therefore,

$$A_{ac} = \begin{bmatrix} 0 & 1 & 0 & 0 & 0 & 0 \\ 0 & 0 & 1 & 0 & 0 & 0 \\ 0 & -\left(\frac{F_1 R_{s1}}{J_1 L_{s1}}\right) & -\left(\frac{F_1}{J_1} + \frac{R_{s1}}{L_{s1}}\right) & 0 & 0 & 0 \\ 0 & 0 & 0 & 0 & 1 & 0 \\ 0 & 0 & 0 & 0 & 0 & 1 \\ 0 & 0 & 0 & 0 & -\left(\frac{F_1 R_{s1}}{J_1 L_{s1}}\right) & -\left(\frac{F_1}{J_1} + \frac{R_{s1}}{L_{s1}}\right) \end{bmatrix}$$

$$B_{ac} = \begin{bmatrix} 0 & 0 \\ 0 & 0 \\ \frac{K_1 R_{s1}}{J_1 L_{s1}} & 0 \\ 0 & 0 \\ 0 & 0 \\ 0 & \frac{K_2 R_{s2}}{J_2 L_{s2}} \end{bmatrix}, \quad Q = \begin{bmatrix} 0 & 0 \\ 0 & 0 \\ -\frac{R_{s1}}{J_1 L_{s1}} & 0 \\ 0 & 0 \\ 0 & 0 \\ 0 & -\frac{R_{s2}}{J_2 L_{s2}} \end{bmatrix}, \quad W = \begin{bmatrix} 0 & 0 \\ 0 & 0 \\ -\frac{1}{J_1} & 0 \\ 0 & 0 \\ 0 & 0 \\ 0 & -\frac{1}{J_2} \end{bmatrix}$$

The parameters of the Brushless DC Motor is as listed in Table 2.1 [Osman,1991].

Table 2.1: Parameters of the Actuators for Robot Arm

Parameter	Notation	Joint(Actuator)	
		1	2
Moment of Inertia	J_i	2.85kg.m ²	1.4kg.m ²
Stator winding resistance	R_{si}	1.2Ω	1.3Ω
Stator winding inductance	L_{si}	0.162H	0.166H
Motor damping constant	F_i	0.0573kg.m ² /s	0.0253kg.m ² /s
Motor torque constant	K_i	19.44N.m/A	12.28N.m/A

2.3 Modeling of Robot Dynamics

The configuration of the direct drive robot arm considered is as shown in Figure 2.4.

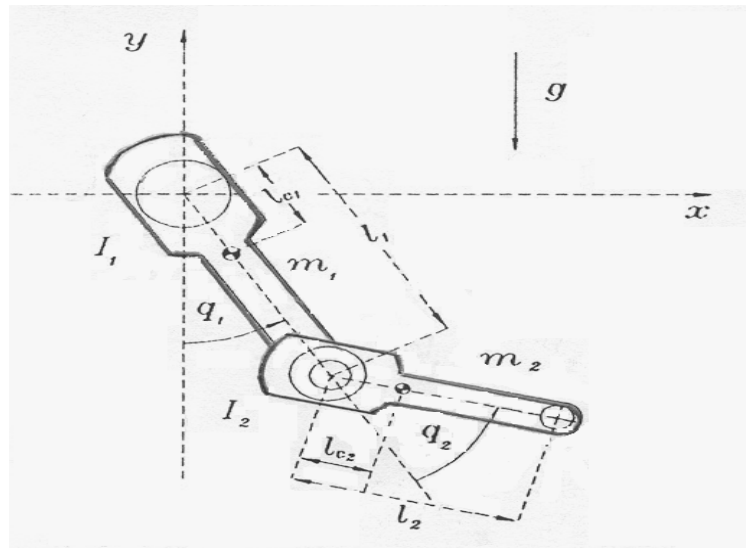


Figure 2.4 : The Configuration of 2 DOF Direct Drive Robot Arm
[Reyes&Kelly, 2001]

The meaning and value of the physical of parameters of this robot arm [Reyes & Kelly, 2001] is as listed in Table 2.2:

Table 2.2 : List of Parameters of Robot Arm

Parameter	Notation	Value
Length link 1	l_1	0.45m
Length link 2	l_2	0.45m
Mass link 1	m_1	23.902kg
Mass link 2	m_2	1.285kg
Link (1) centre of mass	l_{c1}	0.091m
Link (2) centre of mass	l_{c2}	0.048m
Inertia link 1	I_1	1.266kgm ²
Inertia link 2	I_2	0.093kgm ²
Gravity Acceleration	g	9.81m/s ²

The dynamics of a serial 2-link rigid robot shown in Figure 2.4 as follows [Reyes & Kelly,(2001)] :

$$M(q)\ddot{q} + C(q, \dot{q})\dot{q} + g(q) + f(\dot{q}) = T_L \quad (2.4)$$

where;

q = joint displacements,

\dot{q} = joint velocities,

T_L =applied torque inputs,

$M(q)$ = manipulator inertia matrix,

$C(q, \dot{q})$ =matrix of centripetal and Coriolis torques,

$g(q)$ = gravitational torques,

$f(\dot{q})$ =friction torques

Using the robot parameters as tabulated in Table 2.2, the entries for manipulator inertia, centripetal and Coriolis as well as gravitational torque is as follows [Reyes & Kelly,(2001)] :

$$\begin{aligned} M(q) &= \begin{bmatrix} 2.351 + 0.168 \cos(q_2) & 0.102 + 0.084 \cos(q_2) \\ 0.102 + 0.084 \cos(q_2) & 0.102 \end{bmatrix} \\ C(q, \dot{q}) &= \begin{bmatrix} -0.168 \sin(q_2) \dot{q}_2 & -0.084 \sin(q_2) \dot{q}_2 \\ 0.084 \sin(q_2) \dot{q}_2 & 0 \end{bmatrix} \\ g(q) &= \begin{bmatrix} 3.921 \sin(q_1) + 0.186 \sin(q_1 + q_2) \\ 0.186 \sin(q_1 + q_2) \end{bmatrix} \end{aligned} \quad (2.5)$$

Define the system state variables as:

$$\begin{aligned} \ddot{q}_1 &= x_3 & \ddot{q}_2 &= x_6 \\ \dot{q}_1 &= x_2 & \dot{q}_2 &= x_5 \\ q_1 &= x_1 & q_2 &= x_4 \end{aligned} \quad (2.6)$$

Substituting equations (2.6) and (2.5) into equation (2.4) gives :

$$\begin{aligned}
\tau = \begin{bmatrix} \tau_1 \\ \tau_2 \end{bmatrix} &= \begin{bmatrix} 2.351 + 0.168 \cos(x_4) & 0.102 + 0.084 \cos(x_4) \\ 0.102 + 0.084 \cos(x_4) & 0.102 \end{bmatrix} \begin{bmatrix} x_3 \\ x_6 \end{bmatrix} + \\
&\begin{bmatrix} -0.168 \sin(x_4)x_5 + b_1 + \frac{f_{c1} \operatorname{sgn}(x_2)}{x_2} & -0.084 \sin(x_4)x_5 \\ 0.084 \sin(x_4)x_2 & b_2 + \frac{f_{c2} \operatorname{sgn}(x_5)}{x_5} \end{bmatrix} \begin{bmatrix} x_2 \\ x_5 \end{bmatrix} + \\
&\begin{bmatrix} \frac{38.465 \sin(x_1) + 1.8247 \sin(x_1 + x_4)}{x_1} \\ \frac{1.8247 \sin(x_1 + x_4)}{x_1} \end{bmatrix} [x_1] \quad (2.7)
\end{aligned}$$

In the vector-matrix form, equation (2.7) can be represented as follows:

$$\begin{bmatrix} \tau_1 \\ \tau_2 \end{bmatrix} = \begin{bmatrix} a_{11} & a_{12} \\ a_{21} & a_{22} \end{bmatrix} \begin{bmatrix} x_3 \\ x_6 \end{bmatrix} + \begin{bmatrix} b_{11} & b_{12} \\ b_{21} & b_{22} \end{bmatrix} \begin{bmatrix} x_2 \\ x_5 \end{bmatrix} + \begin{bmatrix} c_{11} \\ c_{21} \end{bmatrix} [x_1] \quad (2.8)$$

Equation (2.8) can be rearranged into the following format:

$$T_L = \begin{bmatrix} \tau_1 \\ \tau_2 \end{bmatrix} = \begin{bmatrix} c_{11} & b_{12} & a_{11} & 0 & b_{12} & a_{12} \\ c_{21} & b_{21} & a_{21} & 0 & b_{22} & a_{22} \end{bmatrix} \begin{bmatrix} x_1 \\ x_2 \\ x_3 \\ x_4 \\ x_5 \\ x_6 \end{bmatrix} \quad (2.9)$$

or

$$T_L = M(x).X \quad (2.10)$$

Differentiating equation (2.7) and rearranging it gives the derivative of applied torque inputs:

$$\begin{aligned}
\dot{T}_L = \begin{bmatrix} \dot{\tau}_1 \\ \dot{\tau}_2 \end{bmatrix} = & \begin{bmatrix} 2.351 + 0.168 \cos(x_4) & 0.102 + 0.084 \cos(x_4) \\ 0.102 + 0.084 \cos(x_4) & 0.102 \end{bmatrix} \begin{bmatrix} \dot{x}_3 \\ \dot{x}_6 \end{bmatrix} + \\
& \begin{bmatrix} b_1 - 0.168 \sin(x_4) - 0.168 \sin(x_4) x_5 & -0.084 \sin(x_4) - 0.168 \sin(x_4) x_2 \\ -0.084 \sin(x_4) x_2 & b_2 \end{bmatrix} \begin{bmatrix} x_3 \\ x_6 \end{bmatrix} + \\
& \begin{bmatrix} -0.168 \cos(x_4) x_5 & -0.084 \cos(x_4) x_5 \\ 0.168 \sin(x_4) + 0.084 \cos(x_4) x_2 & 0 \end{bmatrix} \begin{bmatrix} x_2 \\ x_5 \end{bmatrix} + \quad (2.11) \\
& \begin{bmatrix} \frac{38.465 \cos(x_1) - 3.6494 \sin(x_1) \sin(x_4) + 3.6494 \cos(x_1) \cos(x_4)}{x_1} \\ \frac{-3.6494 \sin(x_1) \sin(x_4) + 3.6494 \cos(x_1) \cos(x_4)}{x_1} \end{bmatrix} \begin{bmatrix} x_1 \end{bmatrix}
\end{aligned}$$

Equation (2.11) can be represented as follows:

$$\dot{T}_L = \begin{bmatrix} \dot{\tau}_1 \\ \dot{\tau}_2 \end{bmatrix} = \begin{bmatrix} d_{11} & d_{12} \\ d_{21} & d_{22} \end{bmatrix} \begin{bmatrix} \dot{x}_3 \\ \dot{x}_6 \end{bmatrix} + \begin{bmatrix} e_{11} & e_{12} \\ e_{21} & e_{22} \end{bmatrix} \begin{bmatrix} x_3 \\ x_6 \end{bmatrix} + \begin{bmatrix} f_{11} & f_{12} \\ f_{21} & 0 \end{bmatrix} \begin{bmatrix} x_2 \\ x_5 \end{bmatrix} + \begin{bmatrix} g_{11} \\ g_{21} \end{bmatrix} \begin{bmatrix} x_1 \end{bmatrix} \quad (2.12)$$

or

$$\dot{T}_L = \begin{bmatrix} 0 & 0 & d_{11} & 0 & 0 & d_{12} \\ 0 & 0 & d_{21} & 0 & 0 & d_{22} \end{bmatrix} \begin{bmatrix} \dot{x}_1 \\ \dot{x}_2 \\ \dot{x}_3 \\ \dot{x}_4 \\ \dot{x}_5 \\ \dot{x}_6 \end{bmatrix} +$$

$$\begin{bmatrix} g_{11} & f_{12} & e_{11} & 0 & f_{12} & e_{12} \\ g_{21} & f_{22} & e_{22} & 0 & 0 & e_{22} \end{bmatrix} \begin{bmatrix} x_1 \\ x_2 \\ x_3 \\ x_4 \\ x_5 \\ x_6 \end{bmatrix} \quad (2.13)$$

In general equation (2.13) can be written as

$$\dot{T}_L = P(x) \cdot \dot{X} + R(x) \cdot X \quad (2.14)$$

Substituting equations (2.9) and (2.13) into the equation (2.5) gives

$$\dot{X}(t) = A_{ac} X(t) + B_{ac} U(t) + QM(x) X(t) + W[P(x) \dot{X}(t) + R(x) X(t)] \quad (2.15)$$

Simplification of equation (2.15) provides the integrated dynamic model of the direct drive robot arm :

$$\dot{X}(t) = [1 - WP(x)]^{-1} (A_{ac} X(t) + B_{ac} U(t) + QM(x) X(t) + WR(x) X(t)) \quad (2.16)$$

In general, equation (2.16) can be written as:

$$\dot{X}(t) = A(x) X(t) + B(x) U(t) \quad (2.17)$$

where

$$A(x) = [1 - WP(x)]^{-1} \{A_{ac} + QM(x) + WR(x)\} \quad (2.18)$$

$$B(x) = \{[1 - WP(x)]^{-1} B_{ac}\} \quad (2.19)$$

2.4 The Complete Integrated Model

The complete integrated model of a 2 DOF direct drive robot shown in Figure 2.1 can be obtained by substituting equation (2.10), (2.14), (2.18) and (2.19) into equation (2.17).

$$\dot{X}(t) = \begin{bmatrix} 0 & 1 & 0 & 0 & 0 & 0 \\ 0 & 0 & 1 & 0 & 0 & 0 \\ a_{31} & a_{32} & a_{33} & 0 & a_{35} & a_{36} \\ 0 & 0 & 0 & 0 & 1 & 0 \\ 0 & 0 & 0 & 0 & 0 & 1 \\ a_{61} & a_{62} & a_{63} & 0 & a_{65} & a_{66} \end{bmatrix} \begin{bmatrix} x_1(t) \\ x_2(t) \\ x_3(t) \\ x_4(t) \\ x_5(t) \\ x_6(t) \end{bmatrix} + \begin{bmatrix} 0 & 0 \\ 0 & 0 \\ b_{31} & b_{32} \\ 0 & 0 \\ 0 & 0 \\ b_{61} & b_{62} \end{bmatrix} \begin{bmatrix} U_1(t) \\ U_2(t) \end{bmatrix} \quad (2.20)$$

Therefore,

$$\dot{x}_1(t) = x_2(t)$$

$$\dot{x}_2(t) = x_3(t)$$

$$\dot{x}_3(t) = a_{31}x_1(t) + a_{32}x_2(t) + a_{33}x_3(t) + a_{35}x_5(t) + a_{36}x_6(t) + b_{31}u_1(t) + b_{32}u_2(t)$$

$$\dot{x}_4(t) = x_5(t)$$

$$\dot{x}_5(t) = x_6(t)$$

$$\dot{x}_6(t) = a_{61}x_1(t) + a_{62}x_2(t) + a_{63}x_3(t) + a_{65}x_5(t) + a_{66}x_6(t) + b_{61}u_1(t) + b_{62}u_2(t)$$

where,

$$\begin{aligned} \mathbf{a}_{31} = & 1.07/((-0.03-0.02\cos(x_4))(0.1+0.08\cos(x_4))+1.96+0.06\cos(x_4)) \\ & (0.07(38.47\sin(x_1)+1.82\sin(x_1+x_4))/x_1-0.35(38.47\cos(x_1)- \\ & 3.65\sin(x_1)\sin(x_4)+3.65\cos(x_1)\cos(x_4))/x_1)+(-0.04-0.03\cos(x_4))/ \\ & ((-0.03-0.02\cos(x_4))(0.1+0.08\cos(x_4))+1.96+0.06\cos(x_4))(-0.28\sin(x_1+x_4)/x_1 \\ & -0.71(-3.65\sin(x_1)\sin(x_4)+3.65\cos(x_1)\cos(x_4))/x_1) \end{aligned}$$

$$\mathbf{a}_{32} = 1.07/((-0.03-0.02\cos(x_4))(0.1+0.08\cos(x_4))+1.96+0.06\cos(x_4))$$

$$\begin{aligned} & (-0.16+0.01\sin(x_4)x_5-0.49/x_2+0.06\cos(x_4)x_5)+(-0.04-0.03\cos(x_4))/ \\ & ((-0.03-0.02\cos(x_4))(0.1+0.08\cos(x_4))+1.96+0.06\cos(x_4)) \\ & (-.007\sin(x_4)x_2-0.12\sin(x_4)) \end{aligned}$$

$$\begin{aligned} \mathbf{a33} = & 1.07/((-0.03-0.02\cos(x_4))(0.1+0.08\cos(x_4))+1.96+0.06\cos(x_4)) \\ & (-8.39-0.01\cos(x_4)+0.06\sin(x_4)+0.06\sin(x_4)x_5)+(-0.04-0.03\cos(x_4))/ \\ & ((-0.03-0.02\cos(x_4))(0.1+0.08\cos(x_4))+1.96+0.06\cos(x_4)) \\ & (-0.02-0.01\cos(x_4)+0.06\sin(x_4)x_2) \end{aligned}$$

$$\begin{aligned} \mathbf{a35} = & 1.07/((-0.03-0.02\cos(x_4))(0.1+0.08\cos(x_4))+1.96+0.06\cos(x_4))(0.01\sin(x_4)x_5 \\ & +0.03\cos(x_4)x_5)+(-0.04-0.03\cos(x_4))/((-0.03-0.02\cos(x_4))(0.1+0.08\cos(x_4)) \\ & +1.96+0.06\cos(x_4))(-0.03-0.27/x_5) \end{aligned}$$

$$\begin{aligned} \mathbf{a36} = & 1.07/((-0.03-0.02\cos(x_4))(0.1+0.08\cos(x_4))+1.96+0.06\cos(x_4)) \\ & (-0.01-0.01\cos(x_4)+0.03\sin(x_4)+0.06\sin(x_4)x_2)-7.99(-0.04-0.03\cos(x_4))/ \\ & ((-0.03-0.02\cos(x_4))(0.1+0.08\cos(x_4))+1.96+0.06\cos(x_4)) \end{aligned}$$

$$\mathbf{b31} = 1.07/((-0.03-0.02\cos(x_4))(0.1+0.08\cos(x_4))+1.96+0.06\cos(x_4))$$

$$\mathbf{b32} = (-0.04-0.03\cos(x_4))/((-0.03-0.02\cos(x_4))(0.1+0.08\cos(x_4)) + 1.96+0.06\cos(x_4))$$

$$\begin{aligned} \mathbf{a61} = & (-0.07-0.06\cos(x_4))/((-0.03-0.02\cos(x_4))(0.1+0.08\cos(x_4))+1.96+0.06\cos(x_4)) \\ & (-0.07(38.47\sin(x_1)+1.82\sin(x_1+x_4))/x_1-0.35(38.47\cos(x_1)- \\ & 3.65\sin(x_1)\sin(x_4)+3.65\cos(x_1)\cos(x_4))/x_1)-(-1.82-0.06\cos(x_4))/((-0.03- \\ & 2/95\cos(x_4))(0.1+0.08\cos(x_4))+1.96+0.06\cos(x_4))(-0.28\sin(x_1+x_4)/x_1 \\ & -0.71(-3.65\sin(x_1)\sin(x_4)+3.65\cos(x_1)\cos(x_4))/x_1) \end{aligned}$$

$$\begin{aligned} \mathbf{a62} = & (-0.07-0.06\cos(x_4))/((-0.03-0.02\cos(x_4))(0.1+0.08\cos(x_4))+1.96+0.06\cos(x_4)) \\ & (-0.16+0.01\sin(x_4)x_5-0.49/x_2+0.06\cos(x_4)x_5)-(-1.82-0.06\cos(x_4))/((-0.03- \\ & 0.02\cos(x_4))(0.1+0.08\cos(x_4))+1.96+0.06\cos(x_4))(-0.07\sin(x_4)x_2-0.12\sin(x_4)) \end{aligned}$$

$$\begin{aligned} \mathbf{a63} = & (-0.07-0.06\cos(x_4))/((-0.03-0.02\cos(x_4))(0.1+0.08\cos(x_4))+1.96+0.06\cos(x_4)) \\ & (-8.39-0.01\cos(x_4)+0.06\sin(x_4)+0.06\sin(x_4)x_5)-(-1.82-28/475\cos(x_4))/ \\ & ((-0.03-0.02\cos(x_4))(0.1+0.08\cos(x_4))+1.96+0.06\cos(x_4)) \\ & (-0.02-0.01\cos(x_4)+0.06\sin(x_4)x_2) \end{aligned}$$

$$\begin{aligned} \mathbf{a65} = & (-0.07-0.06\cos(x_4))/((-0.03-0.02\cos(x_4))(0.1+0.08\cos(x_4))+1.96+0.06\cos(x_4)) \\ & (1701/296875\sin(x_4)x_5+14/475\cos(x_4)x_5)-(-1.82-28/475\cos(x_4))/ \\ & ((-0.03-0.02\cos(x_4))(0.1+0.08\cos(x_4))+1.96+0.06\cos(x_4))(-0.03-0.27/x_5) \end{aligned}$$

$$\begin{aligned} \mathbf{a66} = & (-0.07-0.06\cos(x_4))/((-0.03-0.02\cos(x_4))(0.1+0.08\cos(x_4))+1.96+0.06\cos(x_4)) \\ & (-0.01-0.01\cos(x_4)+0.03\sin(x_4)+0.06\sin(x_4)x_2)+0.14(-1.82-28/475\cos(x_4))/ \\ & ((-0.03-0.02\cos(x_4))(0.1+0.08\cos(x_4))+1.96+0.06\cos(x_4)) \end{aligned}$$

$$\mathbf{b61} = (-0.07-0.06\cos(x_4))/((-0.03-0.02\cos(x_4))(0.1+0.08\cos(x_4))+1.96+0.06\cos(x_4))$$

$$\begin{aligned} \mathbf{b62} = & (1.82+0.06\cos(x_4))/((-0.03-0.02\cos(x_4))(0.1+0.08\cos(x_4))+1.96+0.06\cos(x_4)) \\ & (2. \\ & 17 \\ &) \end{aligned}$$

CHAPTER 3

INTEGRAL SLIDING MODE CONTROL DESIGN

3.1 Overview of Controller

Referring to Figure 3.1, control system can be divided into two parts; that are model based and non-model based. Among the well known model based control are adaptive control, computer torque and variable structure control. On the other hand, example of non-model based where knowledge of the mathematical model is not needed are like fuzzy logic, artificial intelligent and neural network. Sliding mode control is a type of variable structure control. It is a robust control and insensitive against uncertainties and disturbances. Integral sliding mode control is a variety of sliding mode control with their own advantages such as no reduced an order of the system and also non-singular transformation to the regular form not needed.

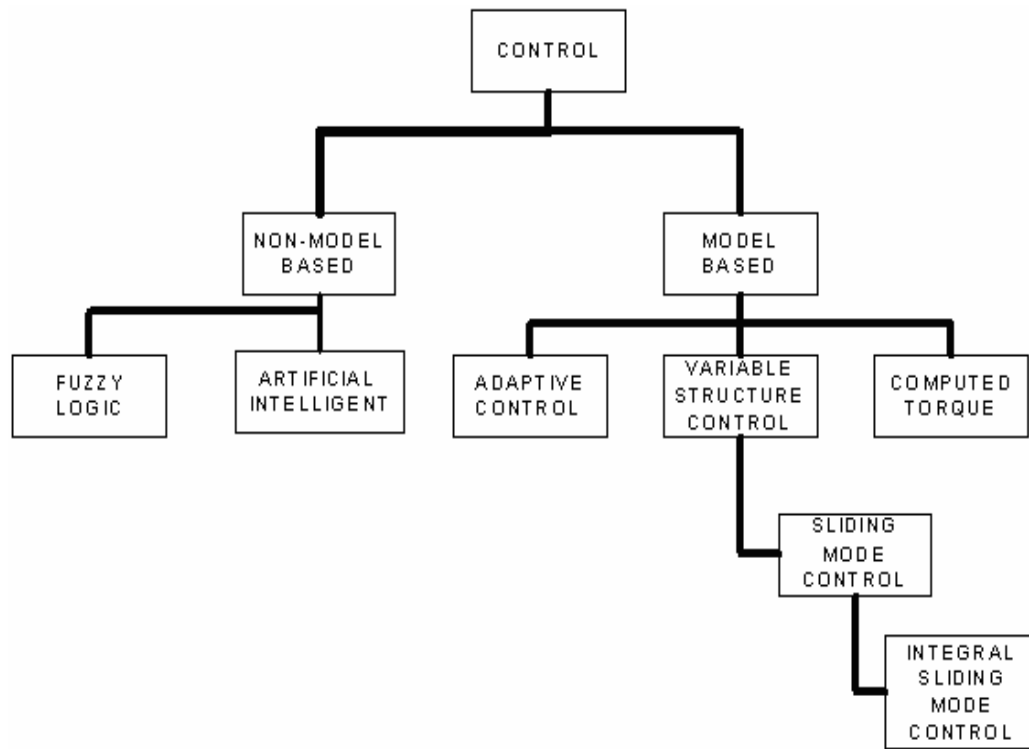


Figure 3.1 : Overview of Control Structure

3.2 Introduction to Variable Structure Control with Sliding Mode Control

One particular approach to robust control controller design is the so-called sliding mode control methodology which is a particular type of Variable Structure Control System (VSCS). Variable Structure Control Systems are characterized by a suite of feedback control laws and a decision rule (termed the switching function) and can be regarded as a combination of subsystems where each subsystem has a fixed control structure and is valid for specified regions of system behavior. The advantage is its ability to combine useful properties of each of the composite structures of the system.

In sliding mode control, the VSCS is designed to drive and then constrain the system state to lie within a neighborhood of the switching function. Its two main advantages are

- a. the dynamic behavior of the system may be tailored by the particular choice of switching function.
- b. the closed-loop response becomes totally insensitive to a particular class of uncertainty. Also, the ability to specify performance directly makes sliding mode control attractive from the design perspective.

The idea of the sliding mode is simple: design a control law with varying control structures, and then force the trajectory of the system state to a certain predefined surface, known as sliding surface, through an appropriate switching of the control structures such that the system dynamics are only determined by the dynamics of the sliding surface.

Sliding Mode Control has for many years been recognized as one of the key approaches for the systematic design of robust controllers for complex nonlinear dynamic systems operating under uncertainty conditions. The major advantage of sliding mode controllers is inherent insensitivity to parameter variations and disturbances once in the sliding mode, thereby eliminating the necessity of exact modeling. Sliding mode control enables separation of the overall system motion into independent partial components of lower dimensions, and as a result reducing the complexity of the control design. The potential of control resources may be used to the fullest extent within the framework of nonlinear control methods since the actuator limitations and other performance specifications may be included in the design procedure.

3.3 Decomposition Into An Uncertain Systems

In order to apply the tracking controller based on the sliding mode control to the direct drive robot arm, the complete integrated dynamics of 2 DOF Direct drive robot given by equation (2.15) need to be decomposed into an uncertain dynamical system as shown below:

$$\dot{X}(t) = [\bar{A} + \Delta A(x, t)]X(t) + [\bar{B} + \Delta B(x, t)]U(t) \quad (3.1)$$

where

$$X(t) = [X_1^T(t) \ X_2^T(t)]^T$$

$$X(t) = [\theta_1(t) \ \dot{\theta}_1(t) \ \ddot{\theta}_1(t)]^T$$

$$U(t) = [U_1(t) \ U_2(t)]^T$$

\bar{A} and \bar{B} are the nominal value of A and B respectively, with

$$\bar{A} = \frac{A_{MAX} + A_{MIN}}{2} \quad (3.2)$$

$$\text{and } \bar{B} = \frac{B_{MAX} + B_{MIN}}{2} \quad (3.3)$$

On the other hand, ΔA and ΔB are uncertainty value of A and B respectively, with

$$\Delta A = \bar{A} - A_{MIN} \quad (3.4)$$

$$\text{and } \Delta B = \bar{B} - B_{MIN} \quad (3.5)$$

The range of x_1, x_2, x_4 and x_5 as below

$$\begin{aligned} 0 \leq x_1 \leq 0.96 & \quad 0 \leq x_4 \leq 3.23 \\ 0 \leq x_2 \leq 2.61 & \quad 0 \leq x_5 \leq 7.63 \end{aligned} \quad (3.6)$$

are used to compute the value of element using equation (2.16).

The nominal matrices A and B as well as the bounds on nonzero element of the matrices can be computed from the maximum and minimum value obtained from equation 3.2, 3.3, 3.4 and 3.5 and the results are tabulated in Table 3.1.

Table 3.1 : Value of Elements in Matrices A(x,t) and B(x,t)

	MAX	MIN	NOMINAL	Δ
a ₃₁	-5.1178	-15.8019	-10.45985	5.34205
a ₃₂	-0.8445	-2.4706	-1.65755	0.81305
a ₃₃	-4.3304	-4.7699	-4.55015	0.21975
a ₃₅	0.122	-0.1288	-0.0034	0.1254
a ₃₆	0.2524	0.0242	0.1383	0.1141
b ₃₁	0.5662	0.5331	0.54965	0.01655
b ₃₂	-0.0034	-0.0324	-0.0179	0.0145
a ₆₁	4.7334	-2.7852	0.9741	3.7593
a ₆₂	0.258	-0.0589	0.09955	0.15845
a ₆₃	0.5279	0.0547	0.2913	0.2366
a ₆₅	-0.0599	-0.1019	-0.0809	0.021
a ₆₆	-0.1345	-0.1363	-0.1354	0.0009
b ₆₁	-0.0069	-0.066	-0.03645	0.02955
b ₆₂	0.9361	0.9321	0.9341	0.002

Substituting the nominal values into equation (2.16) gives the system and input nominal matrices.

$$\bar{A} = \begin{bmatrix} 0 & 1 & 0 & 0 & 0 & 0 \\ 0 & 0 & 1 & 0 & 0 & 0 \\ -10.4599 & -1.6576 & -4.5502 & 0 & -0.0034 & 0.1383 \\ 0 & 0 & 0 & 0 & 1 & 0 \\ 0 & 0 & 0 & 0 & 0 & 1 \\ 0.9741 & 0.0996 & 0.2913 & 0 & -0.0809 & -0.1354 \end{bmatrix} \quad (3.7)$$

$$\bar{B} = \begin{bmatrix} 0 & 0 \\ 0 & 0 \\ 0.5497 & -0.0179 \\ 0 & 0 \\ 0 & 0 \\ -0.0365 & 0.9341 \end{bmatrix} \quad (3.8)$$

The uncertainties for system and input matrices can be obtained by substituting uncertainty value into equation (2.16)

$$\Delta A = \begin{bmatrix} 0 & 1 & 0 & 0 & 0 & 0 \\ 0 & 0 & 1 & 0 & 0 & 0 \\ 5.34205 & 0.81305 & 0.21975 & 0 & 0.1254 & 0.1141 \\ 0 & 0 & 0 & 0 & 1 & 0 \\ 0 & 0 & 0 & 0 & 0 & 1 \\ 3.7593 & 0.15845 & 0.2366 & 0 & 0.021 & 0.0009 \end{bmatrix} \quad (3.9)$$

$$\Delta B = \begin{bmatrix} 0 & 0 \\ 0 & 0 \\ 0.01655 & 0.0145 \\ 0 & 0 \\ 0 & 0 \\ 0.02955 & 0.002 \end{bmatrix} \quad (3.10)$$

3.4 Problem Formulation

Consider the dynamics of the direct drive robot arm as an uncertain system described by equation (3.1).

Define the state vector of the system as

$$X(t) = [x_1(t), x_2(t), \dots, x_n(t)]^T \quad (3.11)$$

Let a continuous function $X_d(t) \in R^n$ be the desired state trajectory, where $X_d(t)$ is defined as:

$$X_d(t) = [x_{d1}(t), x_{d2}(t), \dots, x_{dn}(t)]^T \quad (3.12)$$

Define the tracking error, $Z(t)$ as

$$Z(t) = X(t) - X_d(t) \quad (3.13)$$

In this study, the following assumptions are made:

- i) The state vector $X(t)$ can be fully observed;
- ii) There exist continuous functions $H(t)$ and $E(t)$ such that for all $X(t) \in R^n$ and all t :

$$\Delta A(t) = BH(t) ; \quad \|H(t)\| \leq \alpha \quad (3.14(a))$$

$$\Delta B(t) = BE(t) ; \quad \|E(t)\| \leq \beta \quad (3.14(b))$$

iii) There exist a Lebesgue function $\Omega(t) \in R$, which is integrable on bounded interval such that

$$\dot{X}_d(t) = AX_d(t) + B\Omega(t) \quad (3.15)$$

iv) The pair (A, B) is controllable.

In view of equations (3.13), (3.14) and (3.15), equation (3.10) can be written as an error dynamic system:

$$\dot{Z}(t) = [A + BH(t)]Z(t) + BH(t)X_d(t) - B\Omega(t) + [B + BE(t)]u(t) \quad (3.16)$$

Define the Proportional-Integral (PI) sliding surface as

$$\sigma(t) = CZ(t) - \int_0^t [CA + CBK]Z(\tau) d\tau \quad (3.17)$$

where $C \in R^{m \times n}$ and $K \in R^{m \times n}$ are constant matrices. The structure of the matrix C is as follows:

$$C = \text{diag}[c_1 \ c_2 \ \cdots c_{n_i}] \quad (3.18)$$

where n_i the is the n th state variable associated to the i th input of the system. The matrix

C is chosen such that $CB \in R^{m \times m}$ is nonsingular.

The matrix K is designed to satisfy

$$\lambda_{\max}(A + BK) < 0 \quad (3.19)$$

The control problem is to design a controller using the PI sliding mode given by equation (3.17) such that the system state trajectory $X(t)$ tracks the desired state trajectory $X_d(t)$ as closely as possible for all t in spite of the uncertainties and nonlinearities present in the system.

3.5 System Dynamics During Sliding Mode

Differentiating equation (3.17) gives:

$$\dot{\sigma}(t) = C \dot{Z}(t) - [CA + CBK]Z(t) \quad (3.20)$$

Substituting equation (3.16) into equation (3.19) gives:

$$\dot{\sigma}(t) = CBH(t)Z(t) + CBH(t)X_d(t) - CB\Omega(t) + [CB + CBE(t)]u(t) - CBKZ(t) \quad (3.21)$$

Equating equation (3.21) to zero gives the equivalent control, $U_{eq}(t)$:

$$U_{eq}(t) = [CB + CBE(t)]^{-1} \{CBKZ(t) + CB\Omega(t) - CBH(t)Z(t) - CBH(t)X_d(t)\} \quad (3.22)$$

Noting that

$$[CB + CBE(t)]^{-1} = [(CB)(I_n + E(t))]^{-1} = [I_n + E(t)]^{-1}(CB)^{-1} \quad (3.23)$$

the equivalent control of equation (3.22) can be written as

$$u_{eq}(t) = -[I_n + E(t)]^{-1} \{(H(t) - K)Z(t) - \Omega(t) + H(t)X_d(t)\} \quad (3.24)$$

The system dynamics during sliding mode can be found by substituting the equivalent control (3.24) into the system error dynamics (3.16). After simplification, it can be shown that:

$$\dot{Z}(t) = [A + BK]Z(t) \quad (3.25)$$

Hence if the matching condition is satisfied (equation (3.14) holds), the system's error dynamics during sliding mode is independent of the system uncertainties and couplings between the inputs, and, insensitive to the parameter variations.

3.6 Sliding Mode Tracking Controller Design

The manifold of equation (3.17) is asymptotically stable in the large, if the following hitting condition is held (Ahmad,2003):

$$(\sigma^T(t) / \|\sigma(t)\|) \dot{\sigma}(t) < 0 \quad (3.26)$$

As a proof, let the positive definite function be

$$V(t) = \|\sigma(t)\| \quad (3.27)$$

Differentiating equation (3.26) with respect to time, t yields

$$\dot{V}(t) = (\sigma^T(t) \dot{\sigma}(t)) / \|\sigma(t)\| \quad (3.28)$$

Following the Lyapunov stability theory, if equation (3.26) holds, then the sliding manifold $\sigma(t)$ is asymptotically stable in the large.

Theorem: The hitting condition (3.26) of the manifold given by equation (3.17) is satisfied if the control $u(t)$ of system (3.16) is given by (Ahmad,2003):

$$u(t) = -(CB)^{-1} [\gamma_1 \|Z(t)\| + \gamma_2 \|X_d(t)\| + \gamma_3 \|\Omega(t)\|] SGN(\sigma(t)) + \Omega(t) \quad (3.29)$$

where

$$\gamma_1 > (\alpha \|CB\| + \|CBK\|) / (1 + \beta) \quad (3.30)$$

$$\gamma_2 > (\alpha \|CB\|) / (1 + \beta) \quad (3.31)$$

$$\gamma_3 > (\beta \|CB\|) / (1 + \beta) \quad (3.32)$$

Proof: Substituting equation (3.29) into equation (3.21) gives:

$$\begin{aligned} \dot{\sigma}(t) = & CB[H(t) - K]Z(t) - (CB)[I_n + E(t)](CB)^{-1}\{\gamma_1\|Z(t)\| + \gamma_2\|X_d(t)\| \\ & + \gamma_3\|\Omega(t)\|\}SGN(\sigma(t)) + CBH(t)X_d(t) + CBE(t)\Omega(t) \end{aligned} \quad (3.33)$$

Substituting equation (3.33) into (3.28) gives the rate of change of the Lyapunov function:

$$\dot{V}(t) = \dot{V}_1(t) + \dot{V}_2(t) + \dot{V}_3(t) \quad (3.34)$$

where

$$\dot{V}_1(t) = \frac{\sigma^T(t)}{\|\sigma(t)\|} \{CB[H(t) - K]Z(t) - (CB)[I_n + E(t)](CB)^{-1}\gamma_1\|Z(t)\|SGN(\sigma(t))\} \quad (3.35)$$

$$\dot{V}_2(t) = \frac{\sigma^T(t)}{\|\sigma(t)\|} \{CBH(t)X_d(t) - (CB)[I_n + E(t)](CB)^{-1}\gamma_2\|X_d(t)\|SGN(\sigma(t))\} \quad (3.36)$$

$$\dot{V}_3(t) = \frac{\sigma^T(t)}{\|\sigma(t)\|} \{CBE(t)\Omega(t) - (CB)[I_n + E(t)](CB)^{-1}\gamma_3\|\Omega(t)\|SGN(\sigma(t))\} \quad (3.37)$$

Now let simplify each Lyapunov term as follows. First term of equation (3.35):

$$\begin{aligned} \frac{\sigma^T(t)}{\|\sigma(t)\|} \{CB[H(t) - K]\}Z(t) &\leq \frac{\|\sigma^T(t)\|}{\|\sigma(t)\|} \{\|CB\|\|H(t)\| + \|CBK\|\|Z(t)\| \\ &= \{\alpha\|CB\| + \|CBK\|\}\|Z(t)\| \end{aligned} \quad (3.38)$$

Noting that

$$\frac{\sigma^T(t)}{\|\sigma(t)\|} SGN(\sigma(t)) = \frac{\sigma^T(t)\sigma(t)}{\|\sigma(t)\|^2} = \frac{\sigma^T(t)\sigma(t)}{\left(\sqrt{\sigma^T(t)\sigma(t)}\right)^2} = 1 \quad (3.39)$$

then the second term of (3.35) can be simplified as

$$\begin{aligned} -\frac{\sigma^T(t)}{\|\sigma(t)\|} \{(CB)[I_n + E(t)](CB)^{-1}\gamma_1\|Z(t)\|SGN(\sigma(t))\} &\leq -\|CB\|[\|I_n\| + \|E(t)\|]\|(CB)^{-1}\gamma_1\|Z(t)\| \\ &= -[1 + \beta]\gamma_1\|Z(t)\| \end{aligned} \quad (3.40)$$

Using equation (3.38) and (3.40), equation (3.35) can be written as

$$\dot{V}_1(t) \leq -\{(1+\beta)\gamma_1 - [\alpha\|CB\| + \|CBK\|]\|Z(t)\| \quad (3.41)$$

Similarly, equation (3.36) and (3.37) can be simplified in a same manner and the results are summarized as follows:

$$\dot{V}_2(t) \leq -\{(1+\beta)\gamma_2 - \alpha\|CB\|\|X_d(t)\| \quad (3.42)$$

$$\dot{V}_3(t) \leq -\{(1+\beta)\gamma_3 - \beta\|CB\|\|\Omega(t)\| \quad (3.43)$$

Let (3.30), (3.31) and (3.33) hold, then the global hitting condition (3.26) is satisfied.

CHAPTER 4

SIMULATION RESULTS

4.1 Introduction

A complete set of non-linear dynamic equations of the robot model comprising the mechanical part of the robot and the actuator dynamics have been derived and used in the simulations. The equations are highly non-linear and coupled, taking into account the contributions of the actuator dynamics, as well as the inertias, the Coriolis forces, the centrifugal forces and the gravitational forces present in the mechanical part of the robot arm. These equations were used in the simulation to represent a real direct-drive robot manipulator without any approximation and simplification of the highly non-linear and coupled system. The simulation is carried out by using Matlab/Simulink as a platform.

4.2 Trajectory Generation

A trajectory is defined as a time history of position, velocity and acceleration of each joint of robot arm. The controller is required to track a pre-specified reference trajectory for the joint angle is generated by the cycloidal function, as follows (Osman, 1991):

$$\theta_{di}(t) = \begin{cases} \theta_i(0) + \frac{\Delta_i}{2\pi} \left[\frac{2\pi}{\tau} - \sin\left(\frac{2\pi}{\tau}t\right) \right], & 0 \leq t \leq \tau \\ \theta_i(\tau), & \tau \leq t \end{cases} \quad (4.1)$$

where,

$$\Delta_i = \theta_i(\tau) - \theta_i(0), \quad i = 1, 2 \quad \tau = 2s$$

Figure 4.1 below shows the desired joint angle trajectories for both joints.

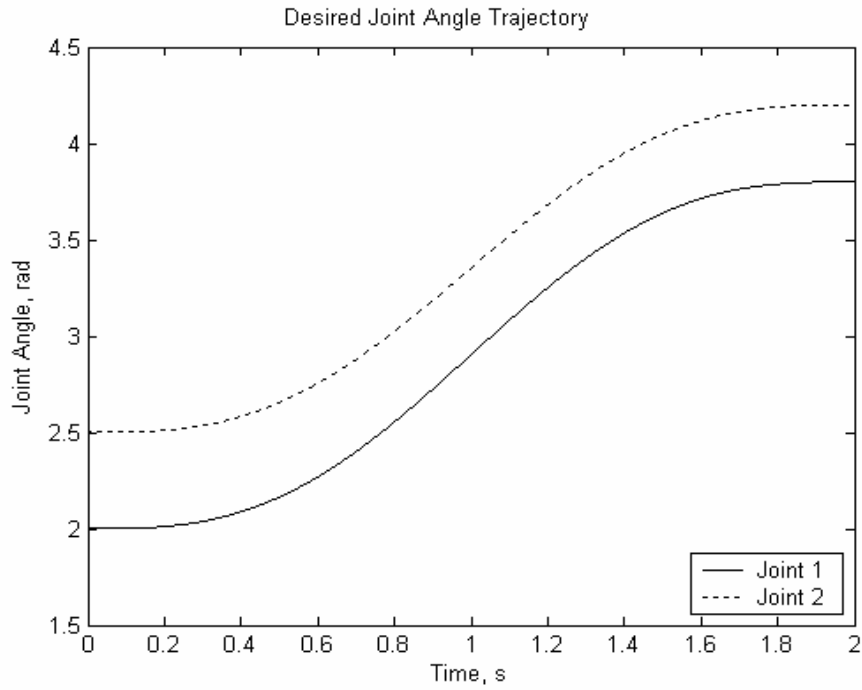


Figure 4.1 Desired Joint Position Profile For Both Joints

By differentiating equation (4.1) with respect to time, t gives the smooth bell shaped velocity profile as shown in the figure 4.2.

$$\dot{\theta}_{di}(t) = \begin{cases} \frac{\Delta_i}{\tau} [1 - \cos(\frac{2\pi t}{\tau})], & 0 \leq t \leq \tau \\ 0 & \tau \leq t \end{cases} \quad (4.2)$$

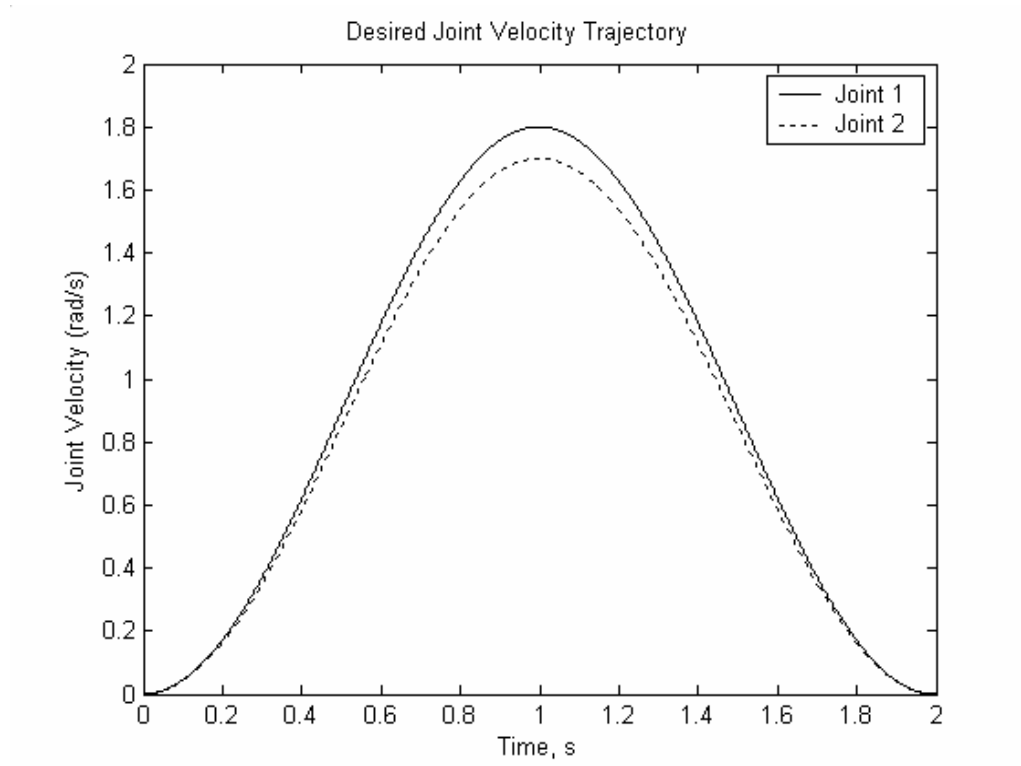


Figure 4.2 : Desired Joint Velocity Profile For Both Joints

The acceleration profile can be generated by differentiating equation (4.2) with respect to time, t . The sinusoidal acceleration profile as follows:

$$\ddot{\theta}_{di}(t) = \begin{cases} \frac{2\pi\Delta_i}{\tau^2} \sin(\frac{2\pi t}{\tau}), & 0 \leq t \leq \tau \\ 0 & \tau \leq t \end{cases} \quad (4.3)$$

Figure 4.3 below shows the desired acceleration profile for both joints of direct drive robot arm.

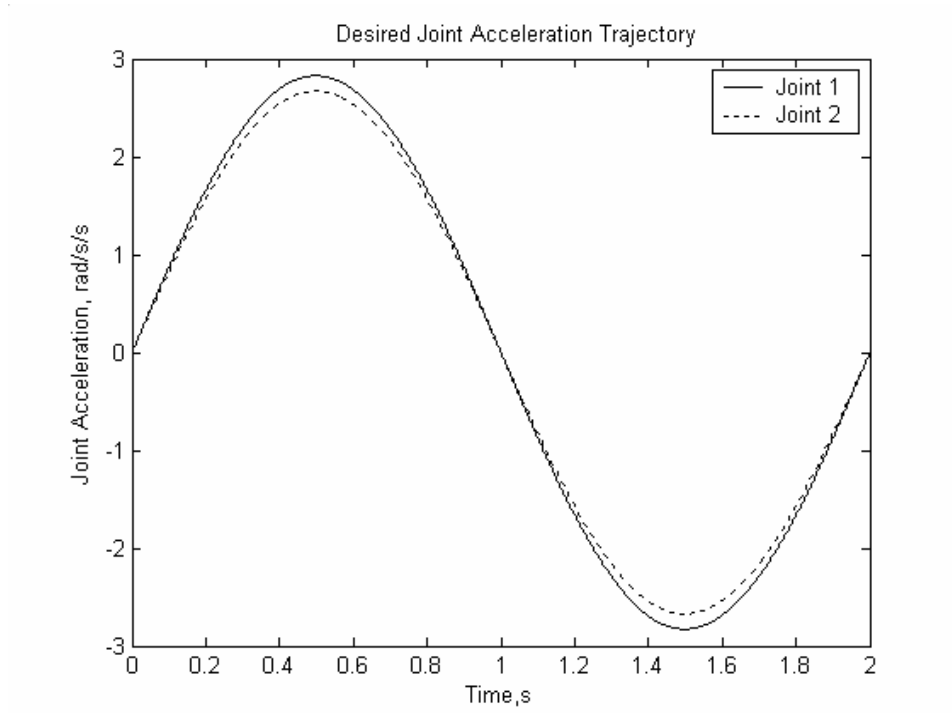


Figure 4.3 : Desired Joint Acceleration Profile For Both Joints

The joint trajectories for both joints are set to start at the initial position of $[\theta_1(0) \quad \theta_2(0)]^T = [-0.8 \quad -1.5]^T$ radians, to a desired final position of $[\theta_1(t) \quad \theta_2(t)]^T = [1 \quad 0.2]^T$ radians in time $\tau = 2$ seconds.

4.3 Simulation Using Independent Joint Linear Control (IJC)

Independent Joint Linear Control method is normally used in most industrial robot. The simulation study is used as comparison to the Integral Sliding Mode Control. Through this simulation, the performance of the IJC can be evaluated when applied to the non linear, time varying and coupled dynamics of the direct drive robot arm.

This controller is designed with the dynamics of the mechanical linkage completely ignored. Each joint of the robot arm is treated as an independent servomechanism problem represented by an actuator state equation as follows:

$$\dot{X}(t) = A_{ac_i} X_i(t) + B_{ac_i} U_i(t) \quad (4.4)$$

The element of matrices A_{ac_i} and B_{ac_i} are similar as described in equation 2.4. Based on the actuator parameters value tabulated in Table 2.1, the matrices A_{ac_i} and B_{ac_i} are calculated as follows:

$$\begin{aligned} A_{ac_1} &= \begin{bmatrix} 0 & 1 & 0 \\ 0 & 0 & 1 \\ 0 & -0.0039 & -7.4275 \end{bmatrix}; \quad B_{ac_1} = \begin{bmatrix} 0 \\ 0 \\ 2.0081 \end{bmatrix} \\ A_{ac_2} &= \begin{bmatrix} 0 & 1 & 0 \\ 0 & 0 & 1 \\ 0 & -0.0039 & -7.8494 \end{bmatrix}; \quad B_{ac_2} = \begin{bmatrix} 0 \\ 0 \\ 3.4343 \end{bmatrix} \end{aligned} \quad (4.5)$$

The linear state feedback controller employed in each of the joint is described as follows:

$$U_i(t) = K_i Z_i(t) + \Omega_i(t) \quad (4.6)$$

where,

K_i - 1x3 linear state feedback gain

$\Omega_i(t)$ - control component to eliminate the steady state error

$$Z_i(t) = X_i(t) - X_{di}(t) \quad (4.7)$$

Each of the sub-system has been assigned with the following closed-loop poles:

$$\lambda_i(A_i + B_i K_i) = \{-2 \quad -1.5 \quad -1\}; \quad i=1,2 \quad (4.8)$$

All desired poles are located in the left half plane to ensure stability.

Using the pole-placement method, the values of feedback gains are obtained as follows:-

$$\begin{aligned} \text{Sub-system 1 : } K_1 &= [1.4939 \quad 3.2349 \quad -1.4578] \\ \text{Sub-system 2 : } K_2 &= [0.8735 \quad 1.8915 \quad -0.9753] \end{aligned} \quad (4.9)$$

The simulation results for Independent Joint Linear Control to track the trajectory of direct drive robot arm for joint 1 and joint 2 are shown in Figure 4.4 and Figure 4.5. From the results that obtained, IJC fails to track the desired positions of both joint 1 and joint 2. The simulation results show that IJC not able handle the highly nonlinear and coupled dynamics of this type of robot arm. In other words, this robot arm requires a more robust controller.

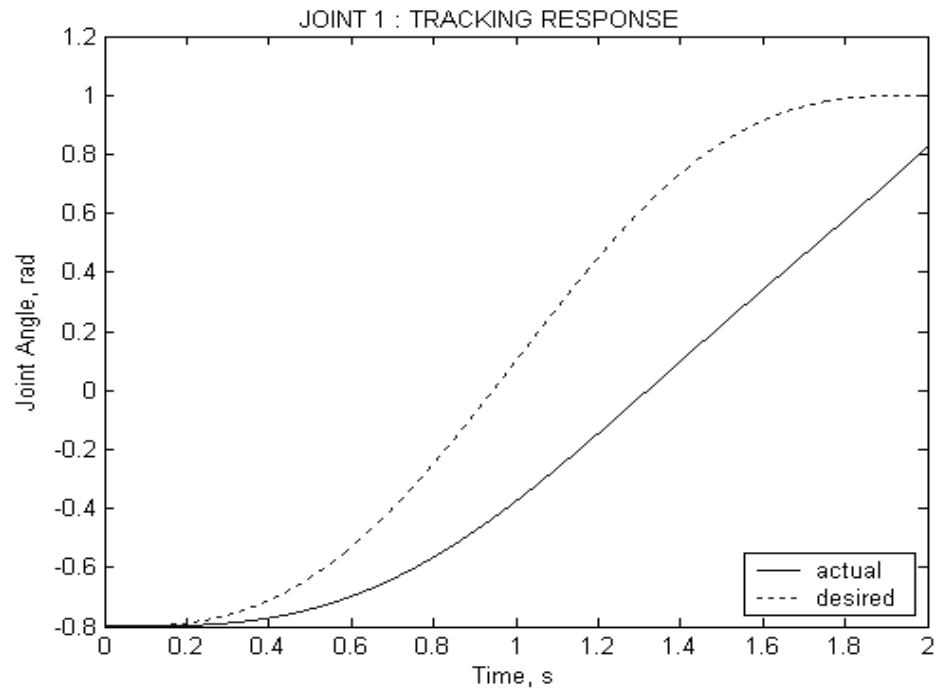


Figure 4.4 : Tracking Response of Joint 1 with IJC

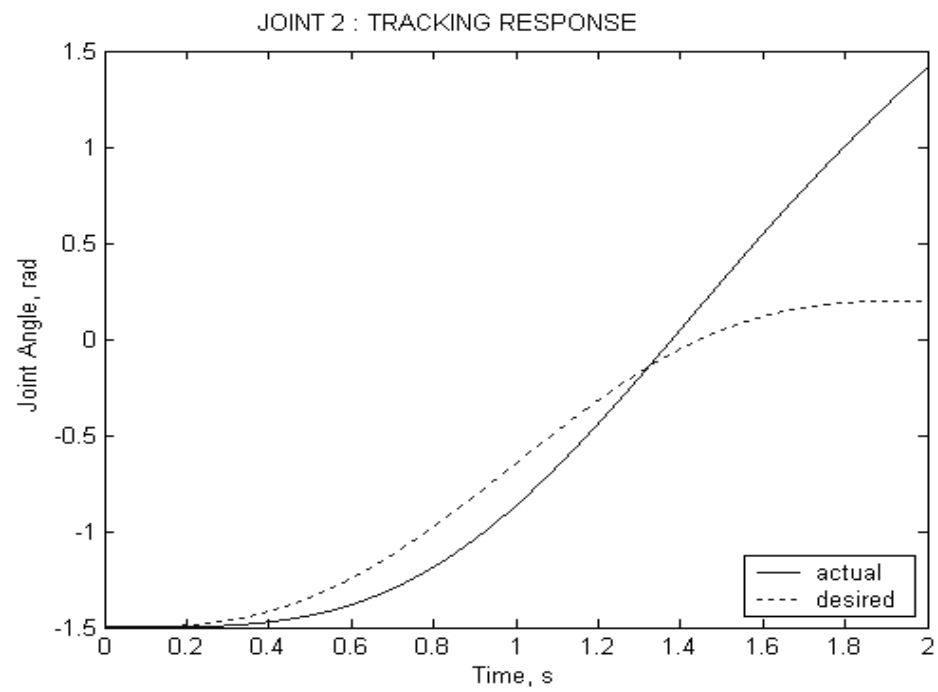


Figure 4.5 : Tracking Response of Joint 2 with IJC

4.4 Simulation Using Integrated Sliding Mode Controller

In this section the simulation is carried out using the controller described by equation (3.29).

4.4.1 The Selection of Controller Parameters

The three values that will determine the shape of the plant output in response to the desired input trajectory are (Ahmad,2003)

a. Sliding Surface Constant, C

The constant c_n , in equation (3.18) will determine the magnitude of the i th input, $U_i(t)$, while the constants $c_1, c_2, \dots, c_{n_i-1}$ will determine the shape of the trajectories during the reaching phase.

b. The Desired Poles Location

The desired poles location can be placed anywhere on the left half plane (LHP) of the s -plane to guarantee stability during the sliding phase. However, if the locations of the desired closed-loop poles are placed too far on the LHP of the s -plane, high gain K will be produced and will somehow affects the shape of the PI sliding surface of equation (3.17).

c. Integral Sliding Mode Controller Parameters, γ

The values of the controller parameters γ_i 's must be large enough to accommodate for the constraint as stated in equations (3.30 – 3.32) but not too large to avoid excessive magnitude of the control input $U_i(t)$.

Although the conditions to achieve desired output response are completely stated as the above, a specific tuning rule for the controller parameters is needed to overcome any constraints that may arise due to the physical limitations of the elements of the system. It is important to note however that the conditions described above can be used to develop an algorithm, which, for each setting of the controller parameters, determines in a systematic way whether the output tracking performance is satisfactory while at the same time guarantee the control input $U_i(t)$ stays within the stipulated limit. The algorithm can be stated as follows (Ahmad, 2003):

Algorithm 4.1 :

Step 1. Input data: Numerical values for $C = \text{diag}[c_1, c_2 \dots c_{n_i}]$,

$$\lambda_{\max}(A + BK) < 0, \text{ and } \gamma_i > 0.$$

Step 2. Check if the sliding mode exists and whether the output tracking response is satisfactory. If the conditions do not hold then try other combinations. If the conditions hold, proceed to **Step 3**.

Step 3. Check if all of the control inputs $U(t) = [U_1(t) \quad U_2(t) \quad \dots \quad U_m(t)]^T$ are within the admissible range. If the condition does not hold then increase the value of c_n , and place the desired poles closer to the origin until sliding mode exist and the control input $U(t)$ is within the admissible limit. If the condition holds, then proceed to **Step 4**.

Step 4. Check if the output trajectories are satisfactory during the reaching phase. If the conditions do not hold then adjust the values of $c_1, c_2 \dots c_{n_i}$ until satisfactory shape of the output trajectories are achieved. If the conditions hold, then proceed to **Step 5**.

Step 5. Check if the tracking errors of the output trajectories are satisfactory. If the conditions do not hold then increase the values of γ_i , for $i = 1, 2, 3$ until satisfactory tracking errors are achieved. The values of γ_i should not be too large to guarantee that the control input $U(t)$ is within the admissible limit. If the conditions hold, then go to **Step 6**.

Step 6. Finish.

The algorithm presented above not only guarantees that the desired tracking response is achieved, but it also assures that the system control input $U(t)$ is within the permissible range of operation.

4.4.2 Numerical Computation

As stated in Chapter 3, the pair (A, B) is controllable. Controllability deals with whether or not the state of a state space equation can be controlled from the input. The pair (A, B) is controllable if for any initial state $x(0) = x_0$ and any final state x_1 , there exists an input that transfers x_0 to x_1 in a finite time. Otherwise (A, B) is said to be uncontrollable (Chi Tsong, 1999). Controllability of the pair (A, B) can be tested by a controllability matrix

$$P_{\Delta} = [B \quad AB \quad A^2 B] \quad (4.10)$$

n - dimensional continuous time system is completely controllable if and only if the matrix has rank n .

By using equation (3.7) and (3.8), the rank of

$$P = \begin{bmatrix} 0 & 0 & 0 & 0 & 0.5497 & -0.0179 \\ 0 & 0 & 0.5497 & -0.0179 & -2.5063 & 0.2106 \\ 0.5497 & -0.0179 & -2.5063 & 0.2106 & 10.5159 & -0.9501 \\ 0 & 0 & 0 & 0 & -0.0365 & -0.9341 \\ 0 & 0 & -0.0365 & 0.9341 & 0.1651 & -0.1317 \\ -0.0365 & 0.9341 & 0.1651 & -0.1317 & -0.6947 & 0.0018 \end{bmatrix} \quad (4.11)$$

is 6, so that the pair (A, B) is controllable.

The bounds of $H(t)$ may be computed as follows using equation (3.14(a))

$$H(t) = [(B^T B)^{-1} B^T] \Delta A(t) \quad (4.12)$$

where, $(B^T B)^{-1} B^T$ is called the pseudo inverse.

Hence,

$$H = \begin{bmatrix} 9.8617 & 1.4865 & 0.4075 & 0 & 0.2291 & 0.2079 \\ 4.4099 & 0.2277 & 0.2692 & 0 & 0.0314 & 0.0091 \end{bmatrix} \quad (4.13)$$

and $\alpha \geq \|H(t)\|$

Therefore,

$$\alpha \geq 10.9223 \quad (4.14)$$

However, the bounds of $E(t)$ may be computed as follows using equation (3.14(b))

$$E(t) = [(B^T B)^{-1} B^T] \Delta B(t)$$

Hence,

$$E(t) = \begin{bmatrix} 0.0312 & 0.0265 \\ 0.0329 & 0.0032 \end{bmatrix}$$

and $\beta \geq \|E(t)\|$

Therefore,

$$\beta \geq 0.0267 \quad (4.11)$$

Define the gain K as:

$$K = \begin{bmatrix} -13.5541 & 8.8239 & -0.0813 & 0.1047 & 0.2179 & 0.4043 \\ 0.5132 & 0.4514 & 0.3087 & 3.2157 & 6.8805 & 4.6883 \end{bmatrix} \quad (4.12)$$

such that the closed-loop poles of the system are:

$$\text{Joint 1: } \lambda_1 = \{-1, -1.5, -2\}$$

$$\text{Joint 2: } \lambda_2 = \{-1, -1.5, -2\} \quad (4.13)$$

The desired poles location can be placed anywhere on the left half plane (LHP) of the s -plane to guarantee stability during the sliding phase

Define the matrix C as:

$$C(t) = \begin{bmatrix} 2 & 3 & 1 & 0 & 0 & 0 \\ 0 & 0 & 0 & 30 & 20 & 1 \end{bmatrix} \quad (4.14)$$

Using (3.34), (3.35) and (3.36), the controller parameter γ may be computed as follows:

$$\gamma_1 > 18.7959; \quad \gamma_2 > 9.9582; \quad \gamma_3 > 0.0243 \quad (4.15)$$

4.4.3 The Effect of the Value of Controller Parameter, γ

The effect of the controller parameter γ is studied in this section. For comparison purposes, two sets of the controller parameters are chosen as shown in Table 4.1:

Table 4.1: Two Sets of Controller Parameters

	Set 1 (Unsatisfied the condition)	Set 2 (Satisfied the condition)
γ_1	10	36
γ_2	5	20
γ_3	0.01	0.875

In Set 1, the controller parameters are selected to study the performance of the system if the controller parameters' conditions of equations (3.34)-(3.36) are unfulfilled, while in Set 2 the controller parameters is selected to represent a situation where the conditions are fulfilled.

The simulation results for both sets are shown in Figure below. From the result obtained, controller fail to track the desired positions if the controller parameters conditions are unsatisfied for joint 1 and joint 2 as shown in Figure 4.6 and 4.7 respectively. This is due to the fact that the control inputs not succeed to switch fast enough and hence the sliding mode fails to materialize. The control input for each subsequent sub-system is shown in Figure 4.8 and 4.9, respectively. . The sliding surfaces of joint 1 and joint 2 are oscillated with large deviations as shown in Figure 4.10 and 4.11, respectively.

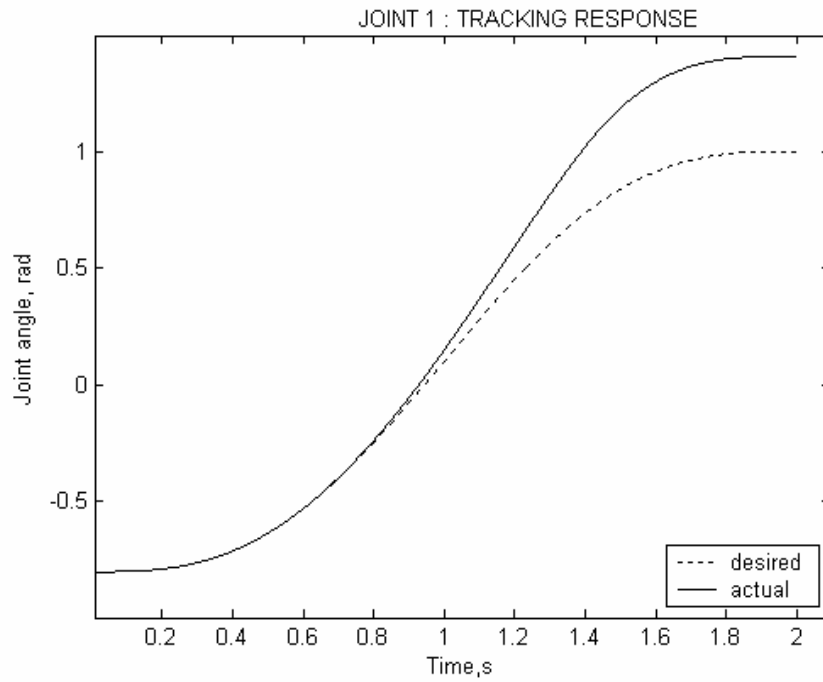


Figure 4.6 : Tracking Response of Joint 1 with Unsatisfied Controller Parameters

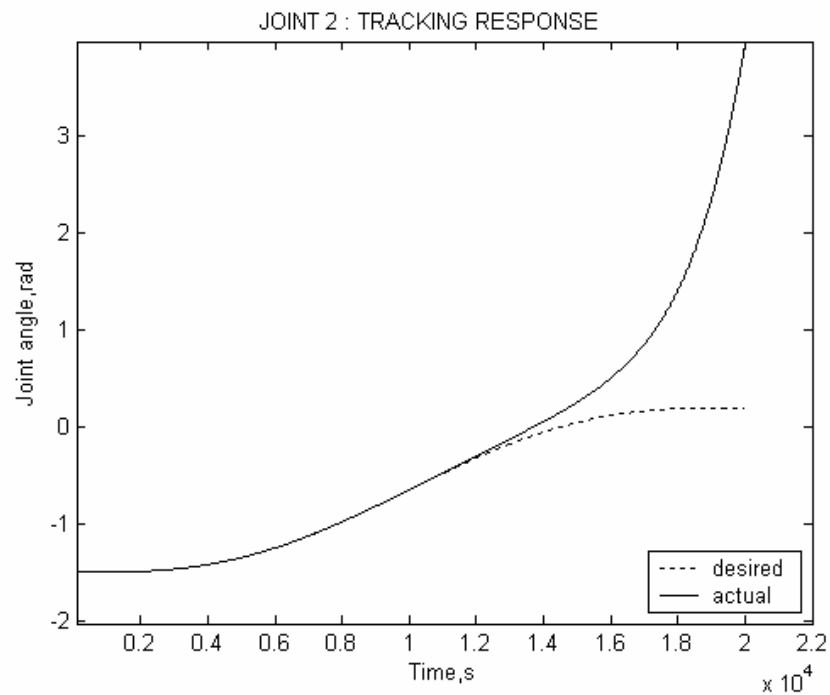


Figure 4.7 : Tracking Response of Joint 2 with Unsatisfied Controller Parameters

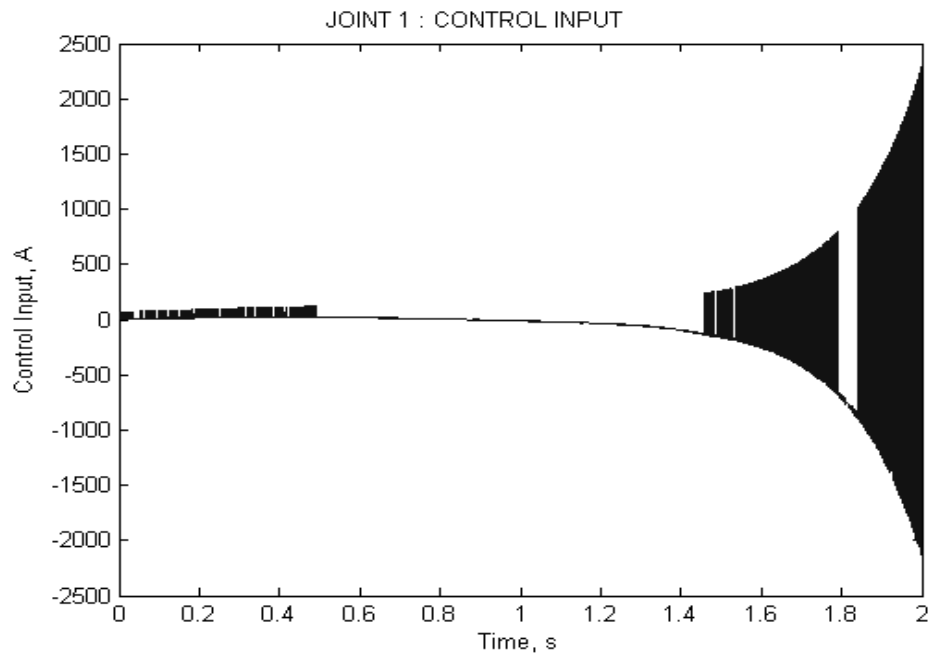


Figure 4.8 : Joint 1 Control Input of PISMIC with Unsatisfied Controller Parameters

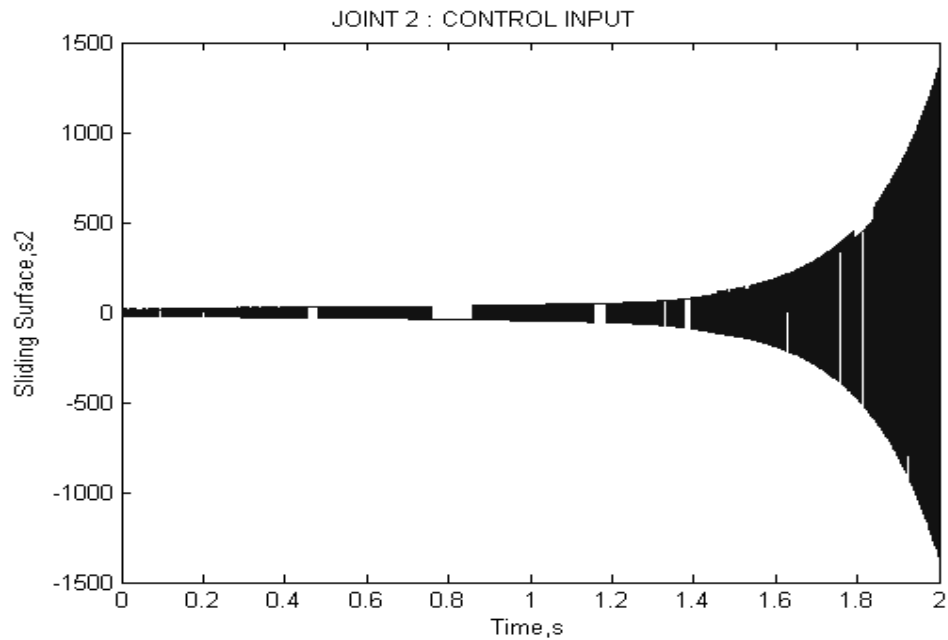


Figure 4.9 : Joint 2 Control Input of PISMIC with Unsatisfied Controller Parameters

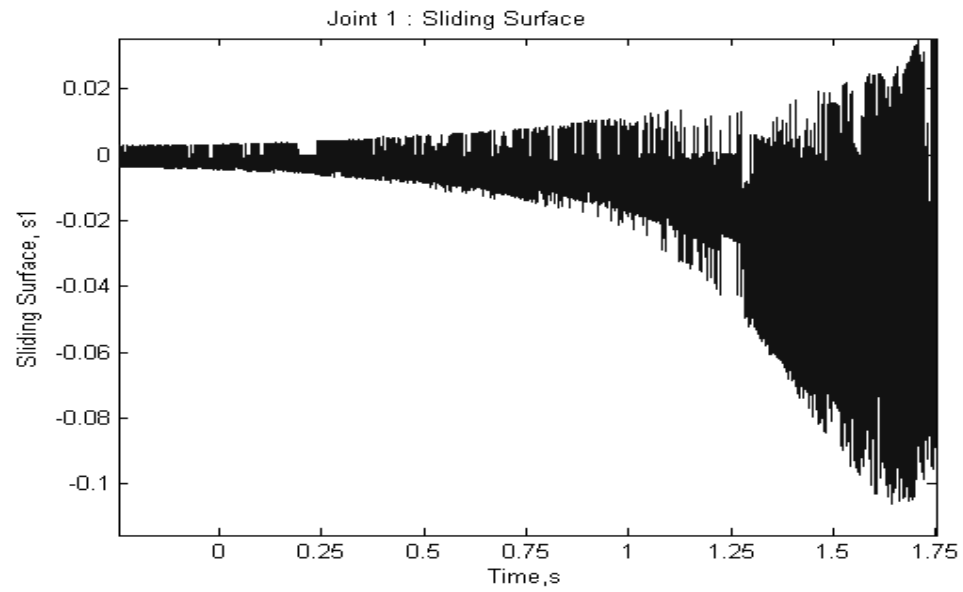


Figure 4.10 : Joint 1 Sliding Surface of PISMIC with Unsatisfied Controller Parameters

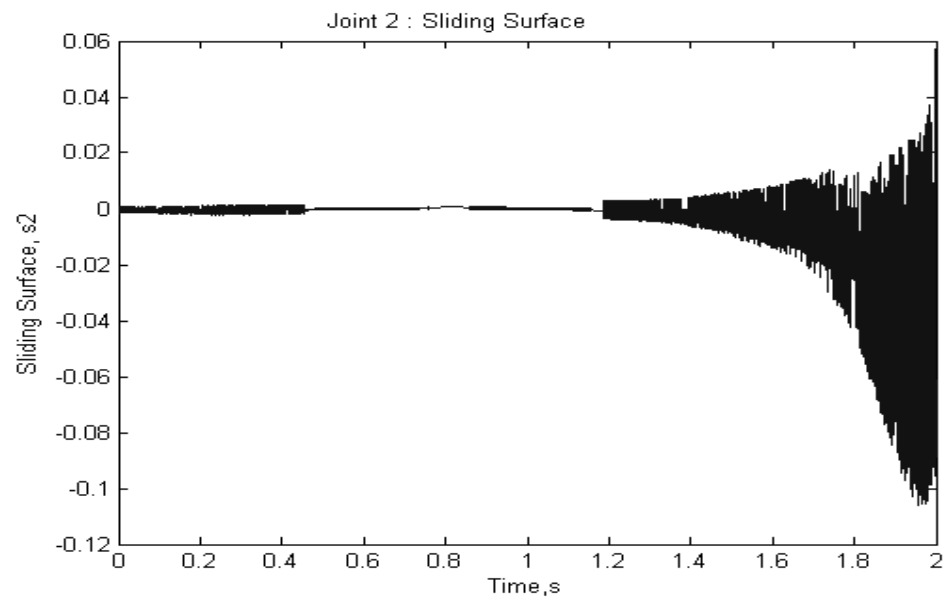


Figure 4.11 : Joint 2 Sliding Surface of PISMIC with Unsatisfied Controller Parameters

However the actual output positions can track the desired trajectory if the controller parameter conditions are satisfied. The good tracking performance results for joint 1 as shown in the Figure 4.12 and for joint 2 as in Figure 4.13. From the result obtained the direct drive robot arm able to track the desired trajectory if the conditions of sliding mode controller parameters are fulfilled. The control input generated for joint 1 and joint 2 switches very fast as shown in Figure 4.14 and 4.15, respectively. . The sliding surfaces of joint 1 and joint 2 as shown in Figure 4.10 and 4.11, respectively.

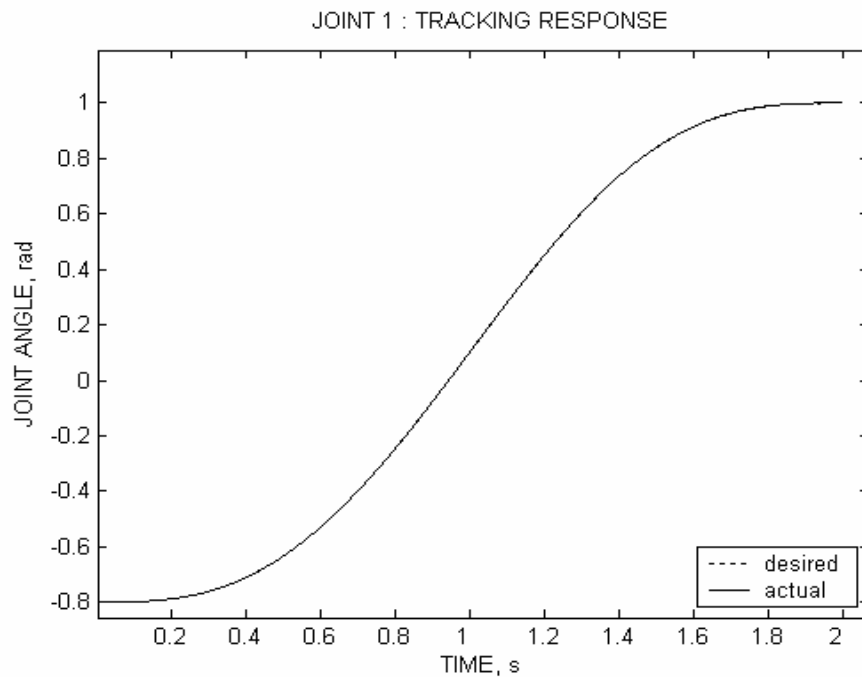


Figure 4.12 : Tracking Response of Joint 1 with Satisfied Controller Parameters

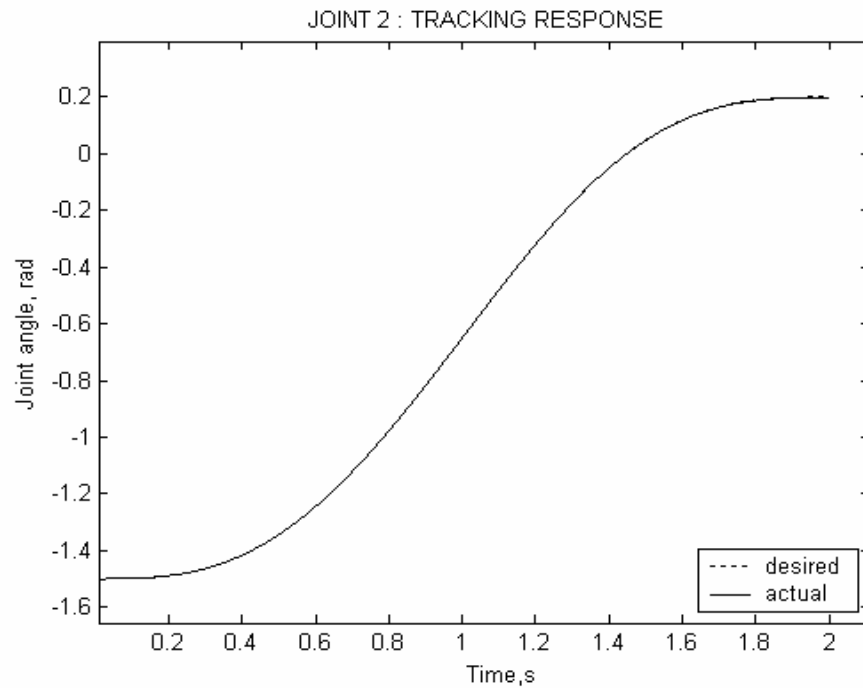


Figure 4.13 : Tracking Response of Joint 2 with Satisfied Controller Parameters

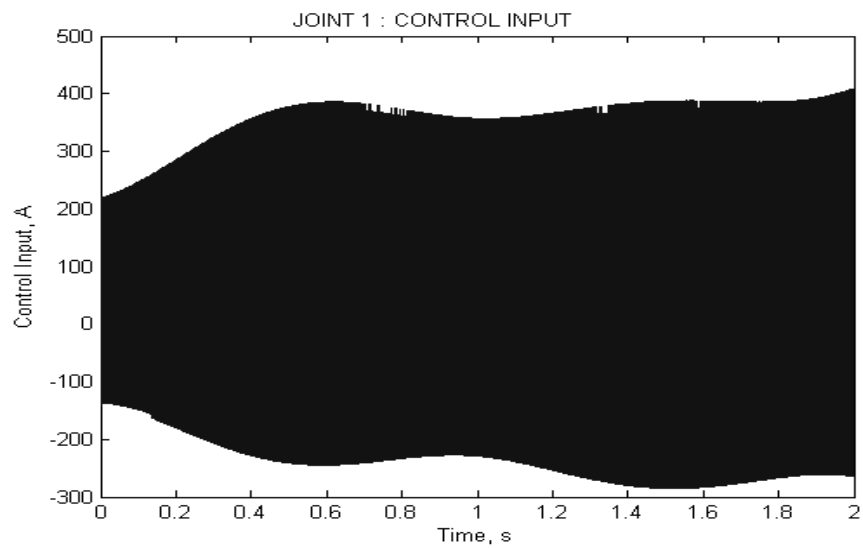


Figure 4.14 : Joint 1 Control Input of PISMCM with Satisfied Controller Parameters

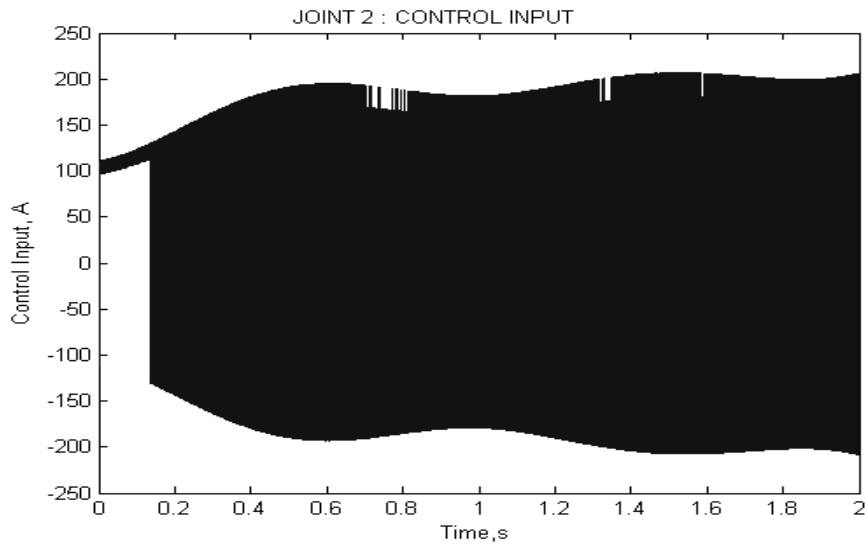


Figure 4.15 : Joint 2 Control Input of PISMIC with Satisfied Controller Parameters

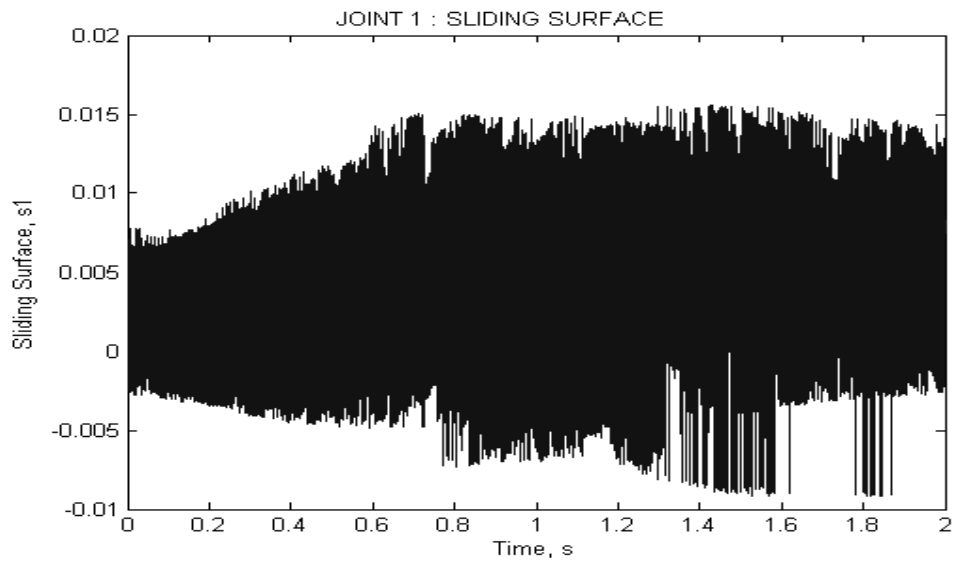


Figure 4.16 : Joint 1 Sliding Surface of PISMIC with Satisfied Controller Parameters

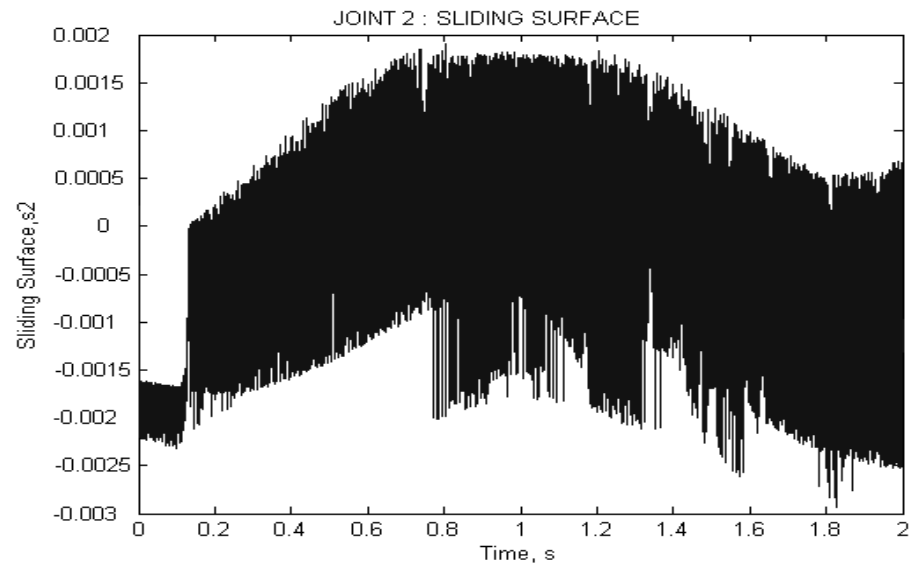
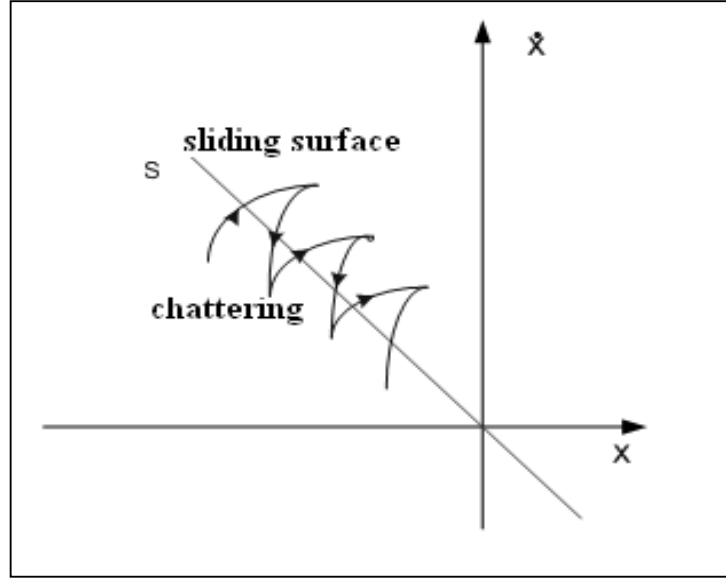


Figure 4.17 : Joint 2 Sliding Surface of PISMIC with Satisfied Controller Parameters

4.6 Control Input Chattering Suppression

In the presence of switching imperfections, such as switching time delays and small time constants in the actuators, the discontinuity in the feedback control produces a particular dynamics behavior in the vicinity of the surface, which is commonly referred to as chattering (Perruquetti and Barbot, 2002). The phenomenon of chattering is shown in Figure 4.18 below. Chattering leads to a high number of oscillations of the system trajectory around the sliding surface, and thus the excessive use of actuators. This will damage the actuators.



The conditions imposed by (3.34), (3.35) and (3.36) not only guarantee that the hitting condition (3.25) is met, but it also assure that based on the Lyapunov theory, the system dynamics is stable in the large.

The sign function $SGN(\sigma(t))$ used in (3.28) is a 2×1 vector of discontinuous functions described as follows:

$$SGN(\sigma(t)) = \begin{bmatrix} SGN(\sigma_1(t)) \\ SGN(\sigma_2(t)) \end{bmatrix}$$

(4.16)

To obtain a continuous control signal such that the control input chattering can be eliminated, each element of the discontinuous sign function $SGN(\sigma(t))$ in (3.28) can be replaced by a proper continuous function (Hashimoto et al, 1987) and (Young, 1988) as follows:

$$S_{\delta_i}(t) = \frac{\sigma_i(t)}{|\sigma_i(t)| + \delta_i} \quad (4.17)$$

where δ_i is a positive constant.

Therefore, in order to eliminate the control input chattering, the discontinuous function vector (4.16) can be replaced by the following continuous function vector:

$$S_{\delta}(t) = \begin{bmatrix} \frac{\sigma_1(t)}{|\sigma_1(t)| + \delta_1} \\ \frac{\sigma_2(t)}{|\sigma_2(t)| + \delta_2} \end{bmatrix} \quad (4.18)$$

This replacement is shown in Figure 4.19. From the figure when δ_i is equal to zero, $S_{\delta_i}(t)$ becomes $SGN(\sigma(t))$ and when δ_i is large, $S_{\delta_i}(t)$ approaches to zero. However if δ_i is small, $S_{\delta_i}(t)$ goes to one.

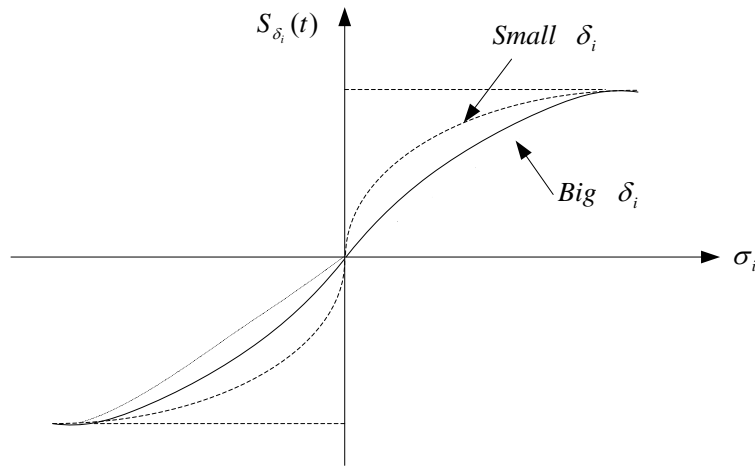


Figure 4.19 : Continuous Function

The continuous function vector (4.18) guarantees that the chattering problem encountered in the control input signal $U(t)$ is removed. This will make the control more sensible from the practical point of view.

To study the behaviour of control input chattering due to the PISMC controller, the simulation settings used in the previous section with the sliding surface constant are simulated again but with the discontinuous function vector $SGN(\sigma(t))$ replaced with a proper continuous functions vector $S_{\delta}(t)$ described by (4.18). The simulation was performed with the continuous function constants δ_i 's are as shown in Table 4.2.

Table 4.2 : Continuous Function Constants

Joint	δ_i	
	1	2
Set 1	2.5	0.25
Set 2	25	2.5
Set 3	250	25

To observe the different between continuous and discontinuous function, the simulation for the both cases is simulated. The control input for joint 1 and 2 using PIMSC with discontinuous function are shown in Figure 4.20 and Figure 4.21, respectively. From the graphs, it can be seen that the chattering occur in the control input for both joints. The magnified figures in the same graphs show that high number of oscillations in the both control input.

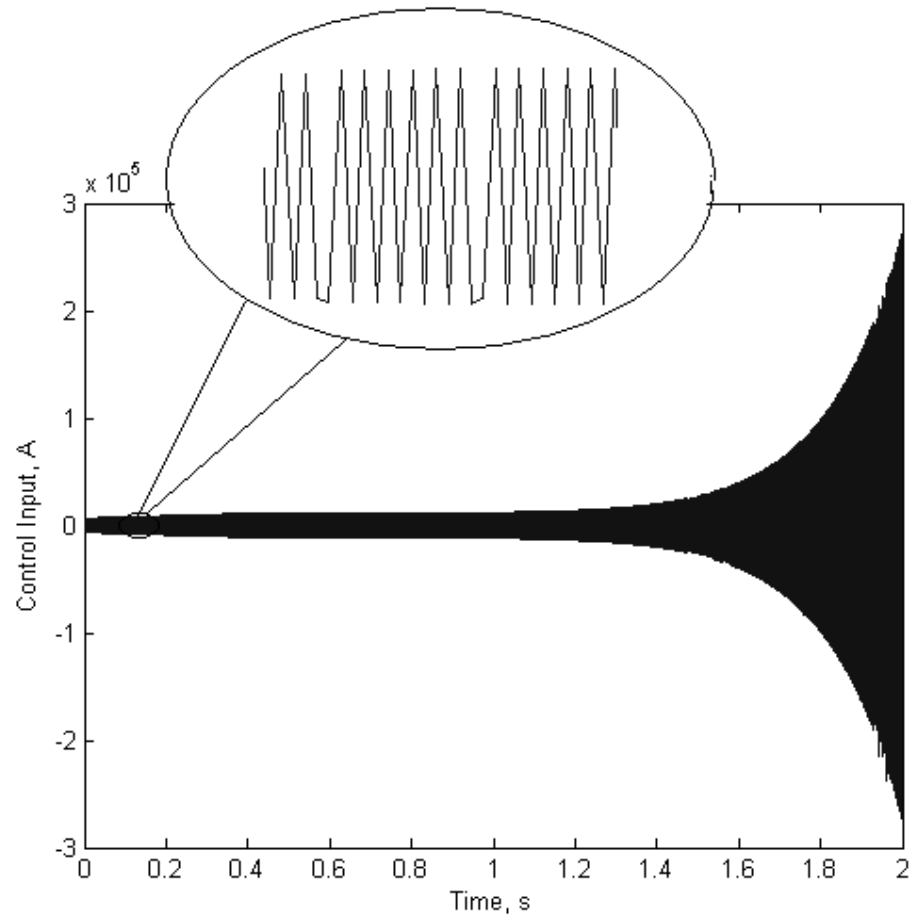


**Figure 4.20 : Joint 1 Control Input Using PISMIC Tracking
Controller with Discontinuous Function**

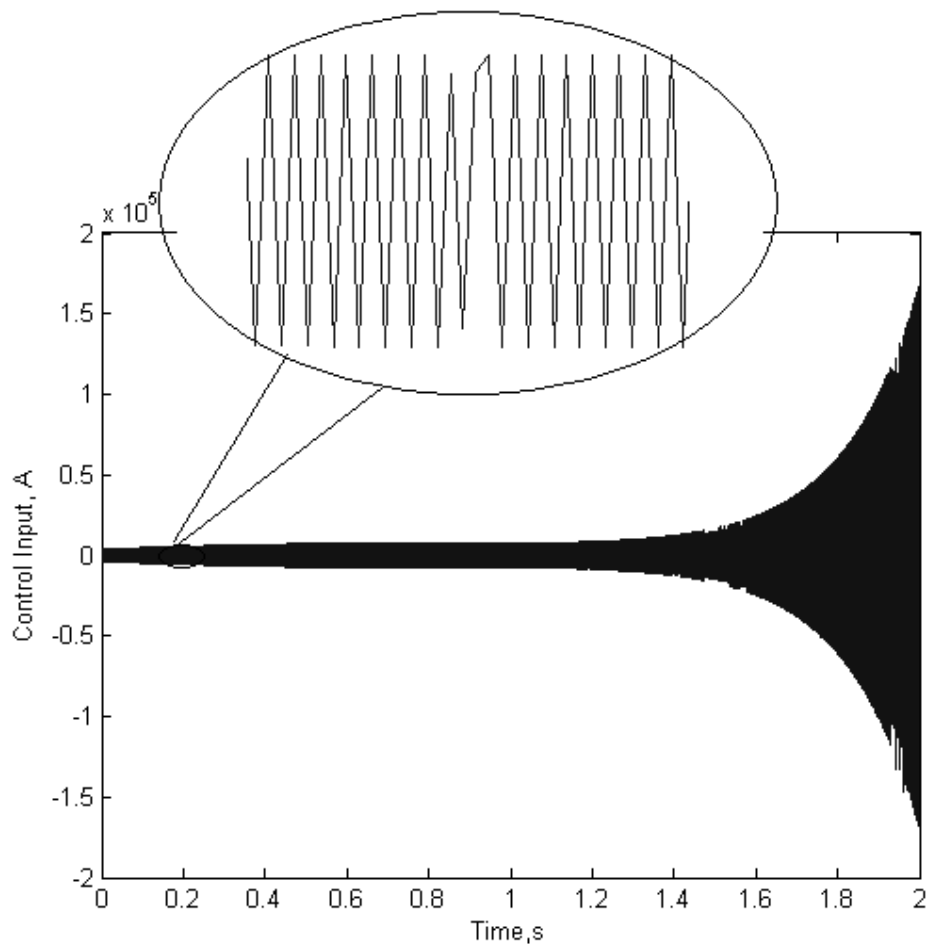


**Figure 4.21 : Joint 2 Control Input Using PISM Tracking
Controller with Discontinuous Function**

The control inputs for joint 1 and joint 2 when the discontinuous function vector $SGN(\sigma(t))$ in (3.28) is replaced by a continuous function vector $S_\delta(t)$ described by (4.18) with its constant δ_i 's tabulated in Table 1 are shown in Figure 4.22 and Figure 4.23, respectively. It can be seen from the graphs that the chattering in the control input is suppressed when the continuous function constant δ_i of set 1 is used. However, δ_i as in Set 2 and Set 3 cannot totally eliminate the control input chattering. In fact this two sets produce tracking errors as can be seen in Figure 4.24 and 4.25. This error will create un-stability in the robot joint tracking response.

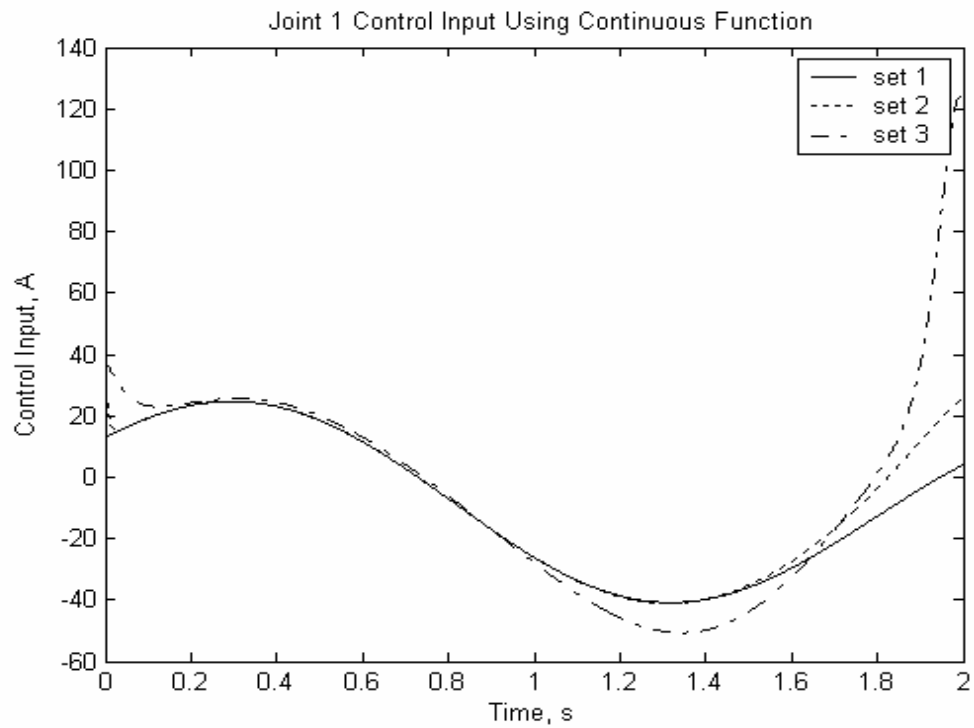


Figure 4.22 : Joint 1 Control Input Using PISM C Tracking Controller with Continuous Function

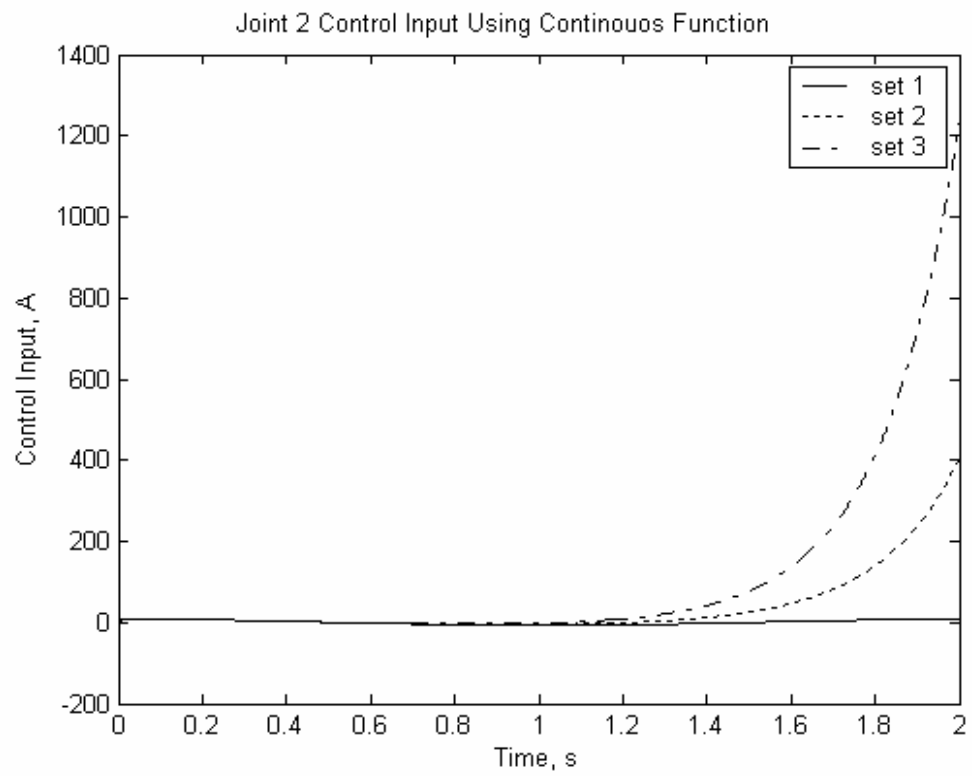


Figure 4.23 : Joint 2 Control Input Using PISM C Tracking Controller with Continuous Function

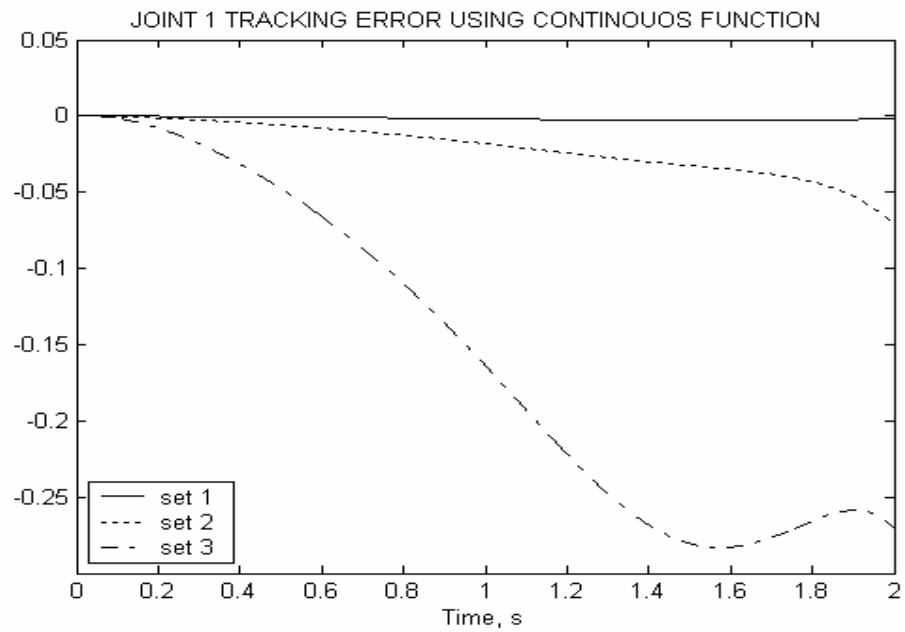


Figure 4.24: Joint 1 Tracking Error Using PISMIC Tracking Controller with Continuous Function

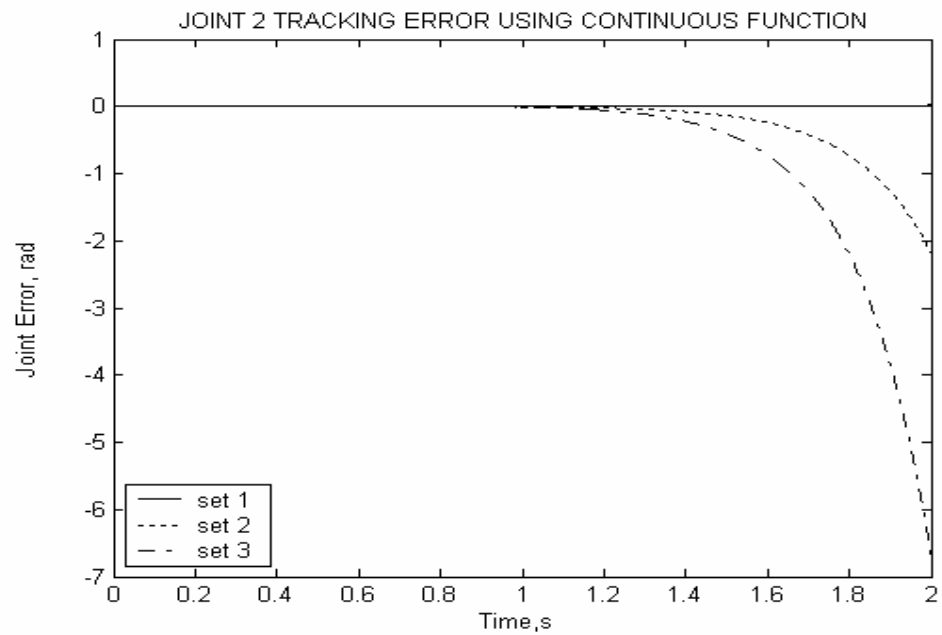


Figure 4.25: Joint 2 Tracking Error Using PISMIC Tracking Controller with Continuous Function

CHAPTER 5

CONCLUSION AND SUGGESTION

5.1 Conclusion

The modelling and control of a 2 DOF direct drive robot arm is presented in this thesis. The formulation of a complete mathematical dynamic model of this direct drive robot arm has been established. The model consists of the dynamics of the mechanical linkage and the dynamics of the actuators. The formulation produces a very nonlinear state equations with input couplings.

This direct drive robot arm requires a robust controller to handle the highly nonlinear and coupled dynamics. Based on variable structure control, an integral sliding mode control as described in Ahmad(2003) is utilized to control the robot arm. However this type of controller introduces a chattering in the input signal. Chattering leads to a high number of oscillations of the system trajectory around the sliding surface, and thus the excessive use of actuators. In this work, chattering is eliminated by replacing the discontinuous function with proper continuous function

For comparison purposes, the robot arm was also simulated independent joint linear control is also analyzed. From the simulation results obtained, linear IJC technique fails to track the desired position. On the other hand, Integral sliding mode control robust against the nonlinearities and uncertainties present in the system and produced very good tracking performance.

5.2 Suggestion For Future Work

The work carried out in this project emphasized on the simulation aspect only. Although the simulation studies on digital computer produced good result, the hardware implementation on a real direct drive robot arm is the way to proceed this project. Through experimental studies, the performance of this controller under real practical environment can be investigated.

REFERENCES

1. Ahmad M.N., (2003). “Modelling And Control Of Direct Drive Robot Manipulators”, Univerti Teknologi Malaysia , PhD Thesis
2. Ahmad M.N., Osman J.H. S., and Ghani M. R. A., (2002) “Sliding Mode Control Of A Robot Manipulator Using Proportional Integral Switching Surface”, *Proc. IASTED Int. Conf. On Intelligent System and Control (ISC2002), Tsukuba, Japan, pp 186-191*
3. An C. H., Atkeson C. G. & Hollerbach J.M., (1988) “Model-Based Control of a Robot Manipulator”, USA: MIT Press.
4. Asada, Kanade& Takeyama, (1983). “Control of a Direct-Drive Arm”. ASME Journal of Dynamic Systems, Measurement, and Control, 105, 136–142.
5. Asada. H & Youcef-Toumi, (1987). “*Direct-Drive Robots: Theory and Practice*”, USA: MIT Press
6. Christopher Edwards and Sarah K. Spurgeon, (1998). “Sliding Mode Control: Theory and Applications”, London: Taylor & Francis Group Ltd
7. John Y. Hung and James C. Hung, (1993).”Variable Structure Control: A Survey”, IEEE Transactions on Industrial Electronics, Vol. 40, No. 1.

8. Karunadasa, J.P., and Renfrew, A.C., (1991). "Design and Implementation of Microprocessor Based Sliding Mode Controller for Brushless Servomotor", IEEE Proceedings-B, Vol. 138, No.6, pp. 345-363.
9. Osman, J.H.S., (1991). "Decentralized and Hierarchical Control of Robot Manipulators." City University, London, UK: PhD . Thesis.
10. Perruquetti W., and Barbot J.P., (2002) "Sliding Mode Control in Engineering", USA :Marcel Decker.
11. R. A. DeCarlo, S. H. Zak and G. P. Matthews, (1988), "Variable Structure Control of Nonlinear Multivariable Systems A Tutorial", *Proc. of the IEEE*, Vol. 76, No. 3.
12. Reyes F. & Kelly R., (2001), "Experimental Evaluation of Model-based Controllers on a Direct-Drive Robot Arm", *Mechatronics*, 11, , 267-282.
13. Young, K-K.D. (1998), "A Variable Structure Model Following Control Design for Robotics Application." *IEEE Journal of Robotics and Automation*, Vol 4, No.5, pp. 556-561.
14. Vadim Utkin, Jurgen Guldner and Jing-Xin Shi, (1999), "Sliding Mode Control in Electromechanical Systems," London: Taylor & Francis Group Ltd,.